Dissertation

submitted to the

Combined Faculties for the Natural Sciences and for Mathematics

of the Ruperto-Carola University of Heidelberg, Germany

for the degree of

Doctor of Natural Sciences

presented by

Diplom-Biochemist Stephan Bernhardt

born in: Dessau, Germany

Oral-examination: 06.11.2017

The Proteomic Landscape of Breast Cancer Metabolism

Referees: Prof. Dr. Stefan Wiemann

PD Dr. Ralf Bischoff

„Borders? I have never seen one. But I have heard they exist in the minds of some people"

Thor Heyerdahl

For my Parents & Jennifer

Declaration of Authorship

I hereby declare that the work presented in my dissertation was carried out from June 2013 to June 2017 under joint supervision of Dr. Ulrike Korf† and Prof. Dr. Stefan Wiemann in the Division of Molecular Genome Analysis at the German Cancer Research Center (DKFZ, Heidelberg, DE).

If not stated otherwise and referenced within the text, the data presented in my dissertation is original, has been performed by myself and has not yet been presented as part of a university examination. Sources that were used and collaborative work have been indicated appropriately. I declare no potential conflict of interest.

Parts of this thesis have been published in:

Bernhardt, S., Bayerlová, M., Vetter, M., Wachter, A., Mitra, D., Hanf, V., Lantzsch, T., Uleer, C., Peschel, S. John, J., Buchmann, J., Weigert, E., Bürrig, K., Thomssen, C., Korf, U., Beissbarth, T., Wiemann, S. and Kantelhardt, E. *Proteomic profiling of breast cancer metabolism identifies SHMT2 and ASCT2 as prognostic factors.* **Breast Cancer Research**, (2017 in revision)

Wachter, A., Bernhardt, S., Beissbarth, T. and Korf, U. *Analysis of Reverse Phase Protein Array Data: From Experimental Design towards Targeted Biomarker Discovery.* **Microarrays** 4, (2015)

Sonntag, J., Schluter, K., Bernhardt, S. and Korf, U. *Subtyping of Breast cancer using reverse phase protein arrays.* **Expert Review of Proteomics** 11, (2014)

Heidelberg,

S. Bernhardt

Acknowledgements

Firstly, I would like to express my deepest gratitude to my former supervisor Dr. Ulrike Korf†. She always encouraged me to pursue my ideas and to embrace scientific resilience. I was deeply saddened to lose a close mentor and extraordinary scientist.

I am very grateful to my supervisor and examiner Prof. Dr. Stefan Wiemann for giving me the opportunity to work in his division, and for the scientific and financial support. He also has been part of my thesis advisory committee (TAC), and took over my supervision in difficult times whilst still providing me with the scientific freedom and encouraging me to work independently.

Furthermore, I would like to thank my other TAC members and examiners, Prof. Dr. Peter Angel, Prof. Dr. Stephan Frings, PD Dr. Ralf Bischoff, Dr. Aurelio Teleman and Prof. Herbert Steinbeisser† for giving me their time and guidance.

My PhD project wouldn't have been possible without collaborations and therefore I like to thank Prof. Dr. Tim Beißbarth and Prof. Dr. Jens Timmer as well as the talented bioinformaticians Dr. Astrid Wachter, Dr. Michaela Bayerlová and Christian Tönsing who have helped me along the way and who performed exceptional analysis for my study.

Likewise, I would like to thank Prof. Dr. Christoph Thomssen, who kindly assisted my collaboration with Dr. Eva Johanna Kantelhardt and Dr. Martina Vetter, who generously supported my PhD project with clinical specimens and clinical information.

Moreover, I thank my fellow PhD students of the Division Molecular Genome Analysis of the German Cancer Research Center for the enjoyable working environment throughout the years and wonderful time also outside the lab.

Finally, I want to thank my girlfriend Jennifer and my family for their constant support and encouragement during my PhD and beyond.

Summary

Breast cancer tumors are recognized to be highly heterogeneous, and differences in their metabolic phenotypes are less well understood. While a number of mostly RNA-based profiling approaches have been developed aiming to improve diagnostic and therapy decision, few have entered clinical practice. Alongside metabolic alterations, tumor hypoxia has consistently been associated with a more aggressive malignant phenotype. Both tumor hypoxia and dysregulated metabolism are classical features of cancer and currently no studies either systematically examine the prognostic value of metabolism associated enzymes in a large cohort of breast cancer patients or their alterations in oxygen deprived conditions.

For my PhD project, I undertook systematic profiling of metabolic enzymes in a cohort of 801 breast cancer patients to evaluate the relationship between profiles of metabolism-associated protein expression and clinicopathological characteristics. I identified three metabolic clusters of breast cancer that are significantly correlated with overall and recurrence-free survival, but do not reflect the common receptor-defined subtypes. Furthermore, high protein expression of the Serine Hydroxy-methyltransferase 2 (SHMT2) and the Amino Acid Transporter (ASCT2), were identified as independent prognostic factors for overall and recurrence-free survival in breast cancer patients.

Another aspect of research revealed the heterogeneous regulation of metabolic enzymes during oxygen deprived conditions and elucidated glutamate-ammonia ligase (GLUL) as a novel effector of the hypoxic response in breast cancer cell lines.

The findings of my thesis are the first to demonstrate metabolic heterogeneity at the protein level in a large breast cancer cohort and highlight the clinical significance of SHMT2 and ASCT2 protein expression as new independent prognostic markers in breast cancer patients. Additionally, GLUL protein expression was identified as a novel effector of the hypoxic rewiring process in breast cancer cell lines. These findings may pave the way for the utilization of SHMT2 and ASCT2 as potential targets for innovative personalized therapy and advance the understanding of metabolic adaptation during hypoxic conditions.

Zusammenfassung

Das Mammakarzinom ist eine heterogene Tumorentität, wobei Unterschiede in Tumormorphologie und deren metabolischen Phänotypen bisher wenig erforscht sind. RNA-basierte Untersuchungstechniken wurden entwickelt, um die Diagnose- und Therapieentscheidung von Brustkrebs Patientinnen zu verbessern, jedoch nur wenige haben Eingang in die klinische Routine gefunden. Neben metabolischen Veränderungen ist auch die Tumorhypoxie mit einem aggressiveren Phänotyp assoziiert. Sowohl Tumorhypoxie, als auch ein dysregulierter Stoffwechsel stellen klassische Merkmale von Krebszellen und Tumoren dar. Derzeit gibt es keine Studien, die die prognostische Aussagekraft Stoffwechsel assoziierter Enzyme in einer großen Kohorte von Brustkrebspatientinnen untersuchen, bzw. die metabolischen Veränderungen in hypoxischen Bedingungen auf breiter Proteinebene abbilden.

Im Rahmen dieser Promotionsarbeit, erfolgte die systematische Untersuchung Metabolismus-assoziierter Enzyme in einer Kohorte von 801 Brustkrebspatientinnen, um die Beziehung zwischen Proteinexpressionen und klinischen bzw. pathologischen Eigenschaften zu bewerten. Drei Cluster konnten identifiziert werden, die signifikant mit dem Gesamt- und Rezidiv-freien Überleben korrelieren, jedoch nicht die Rezeptor-definierten Subtypen reflektieren. Darüber hinaus wird das Ausmaß der Proteinexpression der Serin-Hydroxy-methyltransferase 2 (SHMT2) und des Aminosäure-Transporters (ASCT2) als unabhängige prognostische Faktoren für das Gesamt- und Rezidiv-freie Überleben bei Brustkrebspatienten beschrieben.

Unter hypoxischen Bedingungen konnte zudem eine heterogene Regulation von metabolischen Enzymen gezeigt werden. Hierbei wird die Glutamat-Ammoniak-Ligase (GLUL) als neuer Effektor der hypoxischen Adaption in Brustkrebszelllinien vorgestellt.

Die Ergebnisse meiner Arbeit zeigen erstmals die metabolische Heterogenität auf Proteinebene in einer großen Kohorte und demonstrieren die klinische Bedeutung der SHMT2 und ASCT2-Protein-Expression als neue unabhängige prognostische Marker bei Brustkrebspatientinnen. Basierend auf diesen Ergebnissen können SHMT2 und ASCT2 als potenzielle Kandidaten für innovative personalisierte Therapien weiter untersucht werden. Zusätzlich konnte die Expression von GLUL als neuer Effektor

des hypoxischen Adaptionsprozesses in Brustkrebszelllinien identifiziert und so das Verständnis der metabolischen Anpassung während hypoxischer Bedingungen erweitert werden.

Contents

List of Figures

List of Tables

Chapter 1

Introduction

1.1 Hallmarks of cancer

The Hallmarks of cancer represent acquired features of cancer cells during carcinogenesis. First introduced in 2000 by Hanahan and Weinberg, they comprised limitless replicative potential, evading apoptosis, self-sufficiency in growth signals, insensitivity to anti-growth signals, sustained angiogenesis, tissue invasion and metastasis [1]. Due to extensive research in the field of oncology, more than a decade later, Hanahan and Weinberg revised the classical hallmarks of cancer and added four new additional features. These novel hallmarks represent tumor-promoting inflammation, genome instability, immune system evasion, and dysregulated energy metabolism [2]. Taken together, these functional features of abnormal cell growth, represented in diverse cancer genotypes and phenotypes, are adaptive strategies to overcome specific microenvironmental growth constraints such as hypoxia and enable cancer development [3]. Especially cancer metabolism, as new hallmark of cancer, is of particular interest to my PhD project and its proteomic investigation represents the main part of this thesis (Figure 1).

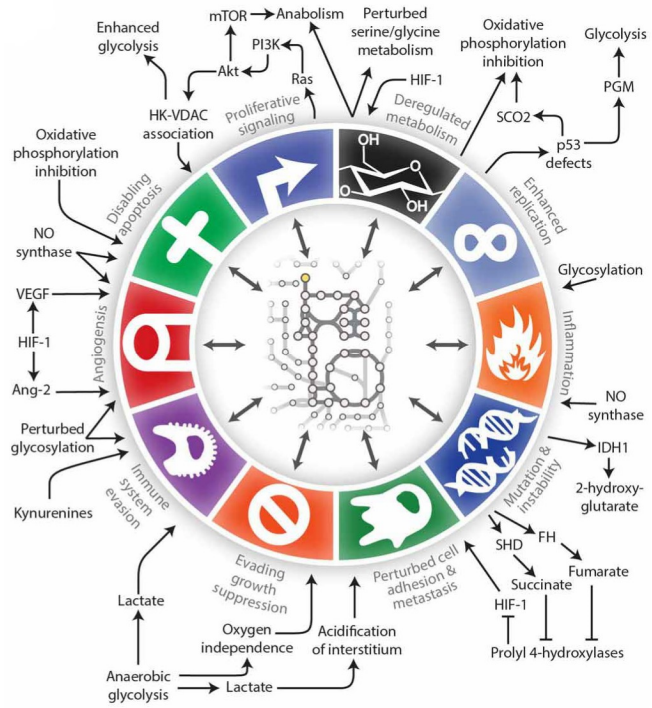

Figure 1 - Hallmarks of cancer: A focus on cancer metabolism.

Hallmarks of Cancer, as illustrated in this figure, are either modulated by metabolic changes or affect metabolism. The schematic overview was adapted from Lewis and Haleem, 2013 [4].

1.2 Breast cancer

1.2.1 Epidemiology, etiology and pathology

Worldwide, breast cancer (BC) is the most prevalent cancer entity among women and commonly known as a heterogeneous disease in terms of tumor morphology and molecular structure [4], [5], [6]. The majority of the increasing incidence of breast cancer cases and deaths, occur in less developed regions with low health expenses per capita. Despite the increase in breast cancer cases, mortality rates have decreased, mainly due to screening programs, earlier detection of the disease, a deeper understanding of the tumor biology, and the development of novel therapeutic strategies for the treatment of patients [7].

The heterogeneity of breast tissue is reflected in its morphology. Surrounded by stromal tissue, the luminal epithelial cells are enveloped by myoepithelial cells that enclose lobules and ducts. Breast cancer refers to several types of neoplasm arising from breast tissue. Differences in the local microenvironment and cellular differentiation states can give rise to phenotypically diverse tumors [8], [9]. Several risk factors like germline mutations, radiation exposure, age, gender, family history, alcohol and obesity have been associated with breast cancer development [10]. The disease is accompanied by a number of symptoms such as a lump in the breast or nipple discharge, and while it is often diagnosed after spread has occurred, the diagnosis at screening (ultrasound or mammography) is increasing [11].

Histologically, breast tumors are classified based on their structural organization and their morphology. Patient tumors are graded based on the degree of cellular pleomorphism, tubular/gland formation, and number of mitoses. Associated with poor outcome are the presence of necrosis, lack of an inflammatory cell reaction, and lymphatic and blood vessel invasion. Furthermore, the presence or absence of lymph node involvement has a strong effect on relapse, rather than the amount of lymph nodes involved [12].

Routine pathological assessment, usually performed by immunohistochemistry (IHC), includes the determination of estrogen receptor (ER) and progesterone receptor (PR) status, which help to predict which patients will benefit from hormonal therapy [13],

[14]. In addition, the human epidermal growth factor receptor 2 (HER2) is also measured as its oncogenic amplification and/or overexpression has an adverse prognostic effect [15]. Cancers overexpressing ER or HER2 are suitable for targeted therapy, like monoclonal antibodies binding to the receptor and disrupting the signaling cascade [16].

1.2.2 Staging and markers of prognosis

Current methods of staging include clinical and pathological information as well as biological assessment. The most commonly used classification is the UICC (International Union Against Cancer) and TNM (Tumor, Node, Metastasis) classification systems, where tumors are classified by size, number of regional lymph nodes and presence or absence of distant metastases [17]. However, the disease course is heterogeneous and while some patients survive for years after developing metastases, others' disease rapidly progresses despite treatment.

The limitations of pathological information for predicting response to treatment, have led to increasing interest in biomarkers such as gene expression signatures and complemented data obtained from histological and immunohistochemical profiling [18]. Gene expression profiling has had a considerable impact in understanding breast cancer biology. During the last decade, intrinsic molecular subtypes of breast cancer (Luminal A, Luminal B, HER2-enriched, Basal-like) and a normal breast-like subgroup have been identified and intensively studied [19]. Recent technological advances and tremendous efforts of consortia like The Cancer Genome Atlas (TCGA) and the Molecular Taxonomy of Breast cancer International Consortium (METABRIC) have further increased our understanding of the molecular pathways and their heterogenous derangements in human solid tumors [20]. A combined evaluation of recurrent gene mutations, gene copy number alterations, and transcriptomic profiles has led to a refinement of the molecular classification of breast cancer (Figure 2). Subtypes can now be defined by multiparameter molecular tests such as the MammaPrint/BluePrint or Prediction Analysis of Microarray (PAM) 50 [21], [22]. However, in clinical practice, the key question is not the separation of molecularly defined intrinsic subtypes, but rather the discrimination between patients who will or will not benefit from particular therapies. Several of the multiparametric

molecular markers have been utilized for this purpose [23], [24]. However, none has received approval in Germany yet for routine testing and therapy decision [25].

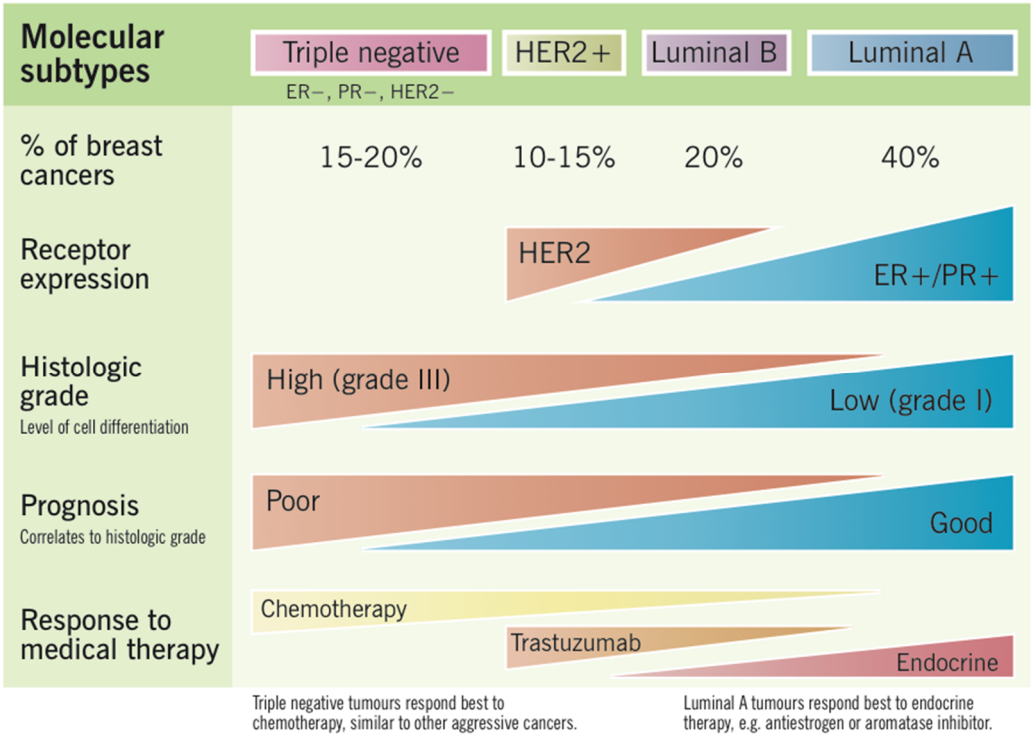

Figure 2 - Breast cancer pathogenesis and molecular subtypes.

This figure was adapted from Sims et al., 2007 [26].

Although many genes and proteins have been investigated as prognostic and predictive factors, only a few are currently decisive for treatment. For now, available predictive models to inform the systemic treatment of individual patients are still limited to a few established biomarkers (mainly hormone receptor and HER2 status, and markers of cell proliferation like Ki67).

A predictive biomarker gives information about the effect of a therapeutic intervention, whilst, a prognostic biomarker provides information about the patient's overall cancer outcome regardless of therapy. So far, just a few predictive biomarkers and signatures like the 'Oncotype Dx' have been evaluated in large scale clinical trials [27], [28].

1.2.3 Treatment and therapy

The current standard of care for patients with primary breast cancer is local management, including surgery and radiotherapy, with or without systemic therapy,

depending on the tumor type and stage. Successful cancer treatment requires the early removal of the tumor cells to prevent recurrence and metastasis, which is the main cause of mortality. If suitable, patients receive neoadjuvant therapy to shrink the tumor before treatment and to allow a breast-conserving surgery. Patients who have no detectable cancer after surgery can be given adjuvant systemic therapy to treat micro metastases.

Stage I and II tumors are usually treated with breast conserving surgery as well as radiotherapy, while Stage III or IV, representing large tumors, may require mastectomy. A systemic therapy may involve hormone treatment, like tamoxifen or aromatase inhibitors and chemotherapy. The treatment protocol depends on stratification factors like patient's age, menopausal status, ER status and HER2 status, Tumor (T) stage, and with increasing prevalence also genomic screening [29]. Please refer to Table 1, adapted from Senkus et al. (2015), for systemic treatment recommendations [30].

Table 1 - Systemic treatment recommendations for breast cancer subtypes

Subtype	Recommended therapy	Comments
Luminal A-like	ET alone in the majority of cases	ChT if: high tumor burden (four or more positive LN, T3 or higher) grade 3
Luminal B-like (HER2-negative)	ET + ChT for the majority of cases	
Luminal B-like (HER2-positive)	ChT + anti-HER2 + ET for all patients	If contraindications for the use of ChT, one may consider ET + anti-HER2 therapy
HER2-positive (non-luminal)	ChT + anti-HER2	
Triple-negative (ductal)	ChT	

ET, endocrine therapy; ChT, chemotherapy; LN, lymph node.

Recently, preclinical studies underline the importance of the immune landscape and point towards the additional benefit of combining treatments aimed at the immune system. Immune-targeted drugs , like PD-1 inhibitors may be suitable in this setting [31]. Another issue based on the broad use of hormonal therapy, is overcoming

endocrine therapy resistance. Combining endocrine agents and blockers of growth factors might be a useful strategy in this context [32].

The heterogeneity of breast cancer is an ongoing challenge for clinicians, as patients with breast cancer and identical clinicopathological characteristics often present markedly distinct outcomes. There is a clear need to identify additional markers to help patient stratification and selecting those patients that may benefit from a certain type of therapy. Therefore, biomarker discovery approaches in areas of the new hallmarks of cancer, like the proteomic exploration of cancer metabolism during my PhD project, might pave the path for a better patient stratification and prognosis evaluation.

1.3 Cancer metabolism

1.3.1 Rewiring of cellular metabolism in cancer

Altered metabolism has been known to characterize tumors ever since Otto Warburg, in the 1920s, reported his first observations of metabolic changes that accompany malignancy [33]. Moreover, deregulated cancer metabolism has regained attention and is regarded as a new hallmark of cancer [34].

Cancer cells differ from healthy cells due to extensive molecular changes, many of which are mechanistically linked to metabolic reprogramming. Proliferative cells as well as tumor cells alter their metabolism in order to support biosynthetic reactions required for accumulation of biomass and the production of macromolecules [35]. Classical features of cancer may be conditioned by metabolic reprogramming, or metabolic reprogramming may be the consequence of nonmetabolic oncogenic events, such as constitutive activation of growth factor pathways, HIF-1 activation, and inactivation of p53 [36]. Moreover, in this context, somatic mutations in oncogenes as well as environmental conditions like inflammation or hypoxia have been shown to cooperate in generating the malignant phenotype [35].

Cancer cells require large amounts of energy and therefore increase their uptake of carbon units with glucose and amino acids as their main sources [35]. Furthermore, oncogenes and tumor suppressors have been shown to directly control many of these adaptations, and consequently, most tumor cells display altered metabolism compared to normal cells [37]. This metabolic rewiring in cancer cells provides a continuous supply of building blocks and supports the production of intermediates for lipid, protein and nucleotide synthesis. Metabolic transformations have been intensively studied over the past decade and as a result, first therapeutic strategies are emerging which target altered metabolism of cancer cells [38].

1.3.2 The Warburg Effect

Historically, the field of cancer metabolism has been rooted in discoveries of the German biochemist Otto Warburg in the 1920s [39]. He and his colleagues observed

that proliferative cells use glycolysis for adenosine triphosphate (ATP) production even in the presence of oxygen and that tumor cells, unlike most normal cells, utilize glycolysis rather than oxidative phosphorylation (OXPHOS) for ATP production (Figure 3). The consequences of this metabolic adjustment are increased glycolytic activity and enhanced lactate secretion, also termed aerobic glycolysis and later known as the "Warburg effect" [34].

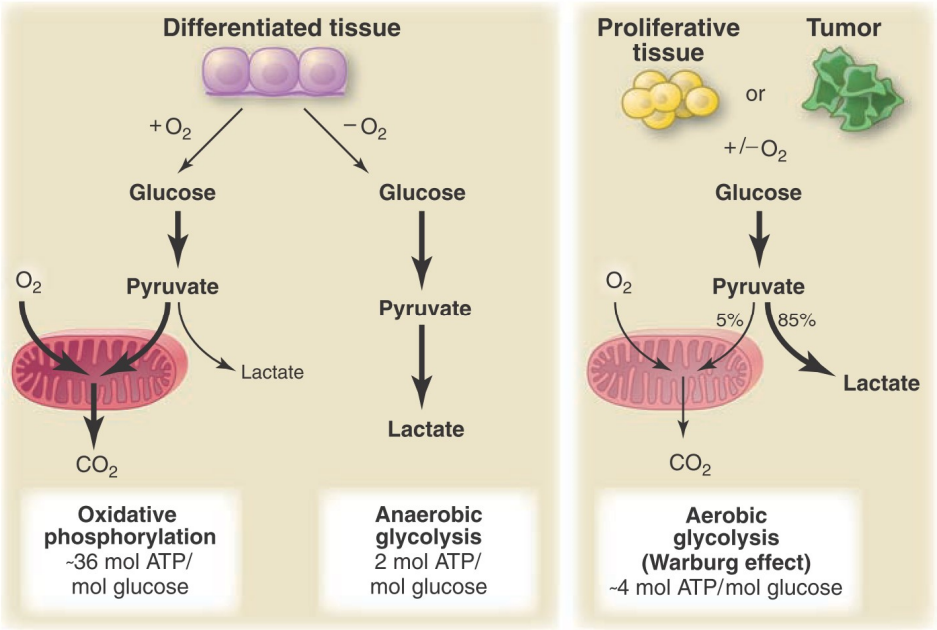

Figure 3 - Energy pathway comparision.

Depicted are differences between oxidative phosphorylation, anaerobic glycolysis, and aerobic glycolysis (Warburg effect). The Figure was adapted from Vander Heiden et al., 2009 [40].

For energy production in normal cells, pyruvate is mainly oxidised in the mitochondria via the tricarboxylic acid cycle (TCA) and under low oxygen conditions, pyruvate is converted into lactate (anaerobic metabolism). Cancer cells primarily use the anaerobic metabolism route. Several explanations have been proposed to describe this phenomenon. Although aerobic glycolysis is less efficient than the OXPHOS in terms of ATP molecules produced per cycle, it has been discussed that tumor cells with glycolytic driven metabolism progress rapidly due to their enhanced glycolytic flux and competitive advantage over their normal counterparts [41]. Since, the production of ATP molecules reaches/exceeds that of oxidative phosphorylation due to the

increased glycolytic flux, the ATP levels meet the demand of highly proliferating cells [40]. Furthermore, lactate, the main end product of aerobic glycolysis provides acidic conditions causing an environment in favour of tumour invasion and suppressing anticancer immune effectors. Cancer cells may also favour aerobic glycolysis over mitochondrial respiration to minimise the generation of reactive oxygen species (ROS). The metabolic re-programming in cancer is essential for redox balance and the synthesis of fatty acids, amino acids and nucleotides to generate macromolecules for cell growth [42], [43]. The extensive increase in glucose uptake by cancer cells also leads to clinical progress in the field of radiology, where glucose uptake is exploited clinically to visualize tumours by 2-(18F)-fluoro-2-deoxyD-glucose positron emission tomography (FDG-PET) [44].

Nevertheless, tumor cells require more than glucose molecules and glycolytic intermediates for their needs to achieve the production of necessary metabolites [45]. In fact, in proliferating cells, glucose alone cannot be used for carbon catabolism and for ATP production. High levels of ATP would impair Coenzyme A production, and consequently another energy source is needed for replenishing the TCA cycle with intermediates for the biosynthesis of macromolecules. In particular, for restoring Oxaloacetic acid levels, which are impaired by the export of citrate from the mitochondria in order to synthesize lipids, tumor cells exploit a different source: glutamine [46].

1.3.3 Glutamine metabolism

After glucose, glutamine represents the most prominent carbon resource for synthesis of the three major classes of macromolecules (Figure 4) [47], [46]. It is also the most abundant amino acid in human plasma and a fundamental source for nucleotide, amino acid and glutathione (GSH) synthesis [48], [49].

The primary functions of glutamine are the storage and transport of nitrogen in the muscle and between organs. Besides its various functions, glutamine is also required for the regulation of the cellular redox potential. Glutamine metabolism provides precursors for the synthesis of GSH, the major thiol containing endogenous antioxidant, which serves as a redox buffer against various sources of oxidative stress. During glutaminolysis, defined as a metabolic process where glutamine is converted to α- ketoglutarate via glutamate, glutamine acts as a nitrogen donor to provide

building blocks for further synthesis of nonessential amino acids [50]. Glutamine itself is traditionally considered a nonessential amino acid, but during periods of rapid growth, the demand for glutamine exceeds its supply and it becomes essential.

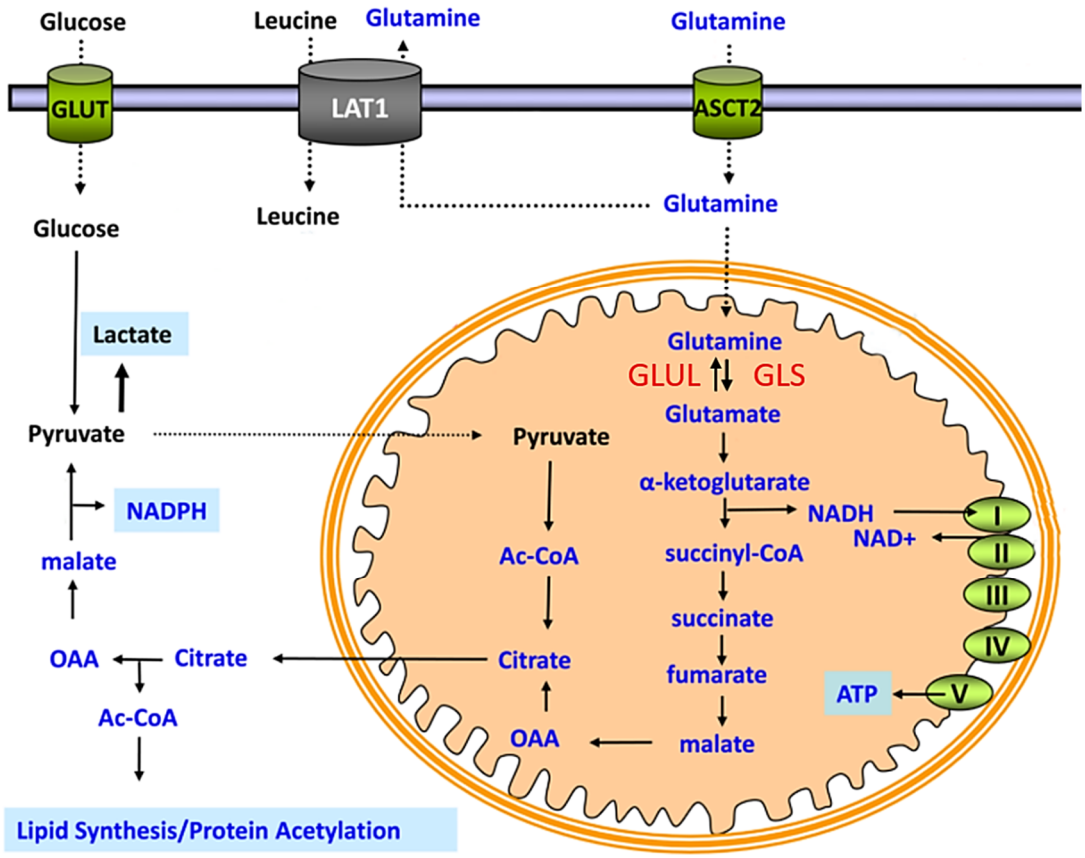

Figure 4 - Glutamine metabolism.

The Figure was modified from Wise et al., 2010 [51]. OAA, Oxaloacetic acid; Ac-CoA, Acetyl-Coenzyme A.

Glutamine can be utilized by the cell to generate the amino acids arginine and proline. In addition to their function as precursors for protein synthesis, proline can act as an antioxidant and arginine is involved in nitric oxide signalling [52], [53]. Moreover, glutamine shuttling across the plasma membrane is necessary for the import of essential amino acids such as phenylalanine [54]. Glutamine itself is transported by several families of amino acid transporters, of which the Na+-dependent ASCT2 transporter, also named SLC1A5 (Solute Carrier Family 1 Member 5), belongs to the most ubiquitously expressed glutamine transporters in human cancer cells [55].

High glucose and glutamine uptake is a common feature of tumor cells and is associated with increased secretion of metabolic by-products such as lactate, alanine and ammonia. [56]. The so-called ‘glutamine addiction’, which is characterized by poor cancer cell survival in the absence of glutamine, has been observed in several cancer entities [57]. Glutamine addicted cells alter their transcriptional programme to upregulate the expression of glutamine transporters and enzymes within the glutaminolysis pathway. Depletion of glutamine prevents the replenishment of TCA cycle metabolites and induces cells to undergo apoptosis. On the contrary, the replenishment of the mitochondrial carbon pool by glutamine provides mitochondria with precursors for the maintenance of mitochondrial membrane potential and for the synthesis of nucleotides, proteins and lipids [58], [59]. Furthermore, glutamine has also been described as an essential activator of the mammalian target of rapamycin complex 1 (mTORC1), which regulates protein translation, cell growth and autophagy [60].

1.3.4 Serine metabolism

Apart from the glutamine metabolism, serine and glycine are also important mediators in cancer cell development. Serine and glycine are biosynthetically linked, and together provide essential precursors for the synthesis of proteins, nucleic acids, and lipids that are crucial to cancer cell growth. Serine hydroxymethyltransferase (SHMT) converts serine to glycine, connecting the serine and glycine pathways. Glycine is required to maintain the cellular redox balance and also sustains oxidative phosphorylation in the mitochondria [61]. It has been shown that glycine uptake and catabolism are able to promote tumorigenesis and malignancy, suggesting that serine and glycine metabolism could in principle be a target for therapeutic intervention [62]. Serine is an important amino acid, not only for protein synthesis, but also for other amino acids, lipids, as well as nucleotide biosynthesis. The endogenous serine synthesis pathway, is the main source of serine in several mammalian tissues, serving also as a source for glycine and one-carbon units for methylation (Figure 5). The upregulation of this pathway has been associated with the ability of breast cancer cells to metastasize [63]. Furthermore, a loss of function screen pointed out that certain breast cancers show PHGDH amplifications and rely on endogenous serine production to sustain proliferation [64]. Interestingly, metabolomics analysis showed that

melanoma and breast cancer cells with PHGDH amplification divert large amounts of glucose-derived carbons into serine and glycine biosynthesis [65].

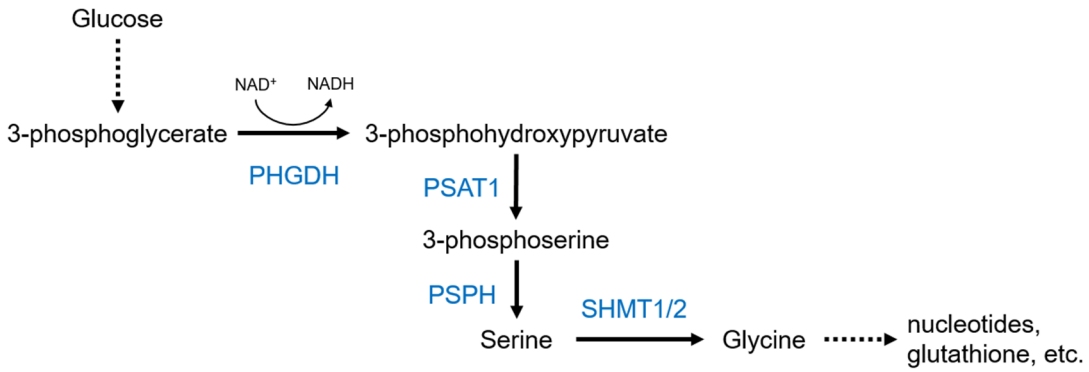

Figure 5 - Serine synthesis pathway.

Scheme of the serine synthesis pathway from glucose and the main biosynthetic pathways in which L-serine is involved. PHGDH, phosphoglycerate dehydrogenase; PSAT1, 3-phosphoserine α- ketoglutarate aminotransferase; PSPH, 3-phosphoserine phosphatase; SHMT1/2, serine hydroxymethyl transferase 1 and 2. Dotted lines indicate multiple step reactions.

In addition to the endogenous serine synthesis pathway, serine metabolism is also important for cancer cells, by contributing to redox balance and glutathione production. Furthermore, p53 has been related to the ability of cells to survive to serine starvation [66], [67].

1.3.5 The role of metabolism in cancer therapy

The increased biosynthetic activity of rapidly proliferating cancer cells provides an 'Achilles heel', as cells depend on the biosynthesis of macromolecules, such as fatty acids, nucleotides and amino acids. During the recent years, it has become clear that altered metabolism could be utilized to develop novel therapeutic approaches and to increase the overall survival of cancer patients. Nowadays, changes of metabolism are investigated in areas of biomarker discovery, patient stratification and drug discovery as well as personalized medicine.

The vast majority of metabolic pathways, which are altered in cancer cells, are also essential for the survival of normal cells and hence are not, in principle, suitable drug targets. However, changes in the activity of a pathway or the presence of a specific enzyme isoform may allow suitable target options. Several studies demonstrate that the metabolic adaptations of cancer cells are not only the consequence of oncogenic

signaling events but can be causally involved in the transformation process. Opinions are emerging that selective pressure can not only alter the activity of metabolic enzymes to enhance the survival of cancer cells, but can also lead to the production of onco-metabolites that may drive tumorigenesis.

Based on these hypotheses, new potential treatment options are emerging. In some tumors, oncogenic BRAF and RAS mutations have been associated with increased GLUT1 expression and specific GLUT1 inhibitors are currently being explored in clinical trials [68], [69]. Another example, addressing the increased lactate production of cancer cells, is the PDK inhibitor DCA (Dichloroacetate), that showed anti-cancer effects in pre-clinical studies and it is already a prescription drug for the treatment of lactic acidosis and well tolerated in patients with glioblastoma multiforme (GBM) [70]. However, neither DCA nor other PDK inhibitors have been approved yet for cancer therapy. A number of therapeutic strategies that target upstream regulators of metabolic pathways, like the hypoxia response factor HIF and the PI3K/AKT signaling cascade, are also emerging as potential targets of interest [71], [72].

Tumor growth is not only characterized by uncontrolled proliferation but also by changes in the microenvironment of the cancer cells. Moreover, the tumor microenvironment itself can impact tumor metabolism and affect the metabolic activity of cancer cells. The increased nutrient influx into cancer cells and their enhanced metabolic rate also leads to an increase in metabolic by-products that are secreted into the surrounding tissue. In order to remove any toxic by-products, tumor cells need profound mechanisms that can stabilize their intracellular as well as their extracellular environment. One of these metabolic adaptations due to changes in the microenvironment is represented in the metabolic rewiring in oxygen deprived conditions, like tumor hypoxia.

1.4 Tumor hypoxia

1.4.1 Tumor hypoxia and microenvironment

Tumor hypoxia is characterized as an insufficient oxygen supply for metabolic needs of the cell and has been shown to be an independent adverse prognostic factor in many cancers, including breast cancer [73]. The negative effect of tumor hypoxia on survival is displayed in two ways. On the one hand, limited effectiveness of radiation therapy leads to less oxygen free radicals generated by ionizing radiation that can cause DNA damage such as cross linkages and double-strand breaks [74]. On the other hand, hypoxic cells can be chemo resistant due to decreased drug action in the absence of oxygen, cell cycle changes, or altered pH gradients [75].
Hypoxia in solid tumors arises from changes in the tumor vasculature such that oxygen demands exceed supply (Figure 6).

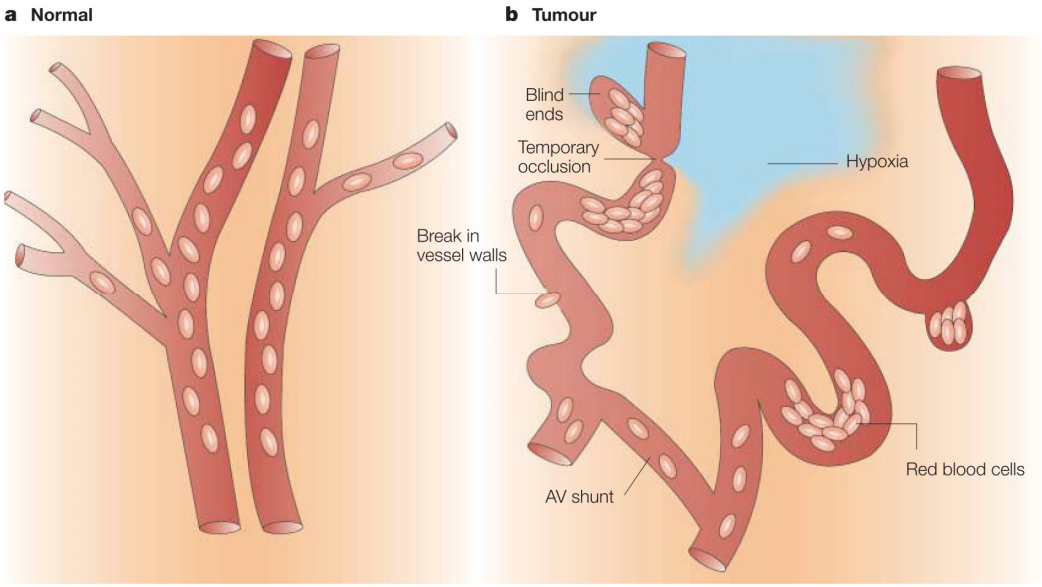

Figure 6 - The vascular network of normal tissue versus tumor tissue.

The picture shows the vascular network of normal tissue (a) and tumor tissue (b). The Figure was adapted from Brown et al., 2004 [76]. AV, Arteriovenous.

These abnormalities arise mainly from a rapidly growing tumor, inefficient alignment of capillaries, low partial pressure (pO_2) in regions distant from arteriolar origin, low vascular density, and variations in capillary red blood cell flux [76].

A key factor of hypoxia is the activation of gene expression pathways to control angiogenesis, resistance to oxidative stress, the switch to anaerobic metabolism, metastasis, and to enhance survival of tumor cells after therapy [77]. Conditions of very severe hypoxia are commonly called anoxia and also reflect the morphology in tumors. In response to anoxia, cells induce cryoprotective programs and stress response to protect key cellular components by reducing translation, increasing expression of endoplasmic reticulum chaperones and arresting in G1 phase of the cell cycle [78].

Compared to room air oxygen with a pO_2 of approximately 159 mmHg, the pO_2 in arterial blood reaches approximately 40 mmHg, and most normal tissues show levels of above 20 mmHg. A partial pressure of less than 10 mmHg, generally induces genes regulated by the hypoxia-inducible transcription factor which is further discussed in the next section. Some normal tissues like primitive stem cells in the bone marrow are hypoxic *per se* and are maintained in a quiescent state by hypoxia-related proteins. Tumors show a heterogeneous picture in oxygen status and frequently display large hypoxic areas (in approximately 60% of solid tumors) with pO_2 median values across the tumor of less than 10 mmHg [79].

Hypoxic experiments referred to in this thesis were performed at 21%, 1,2% or 0.2% oxygen and are roughly equivalent to pO_2 of 159 mmHg, 9 mmHg and 1.5 mmHg respectively.

1.4.2 Hypoxia-inducible factors and their role in cancer

Hypoxia inducible transcription factor 1 (HIF-1) is a key regulator of the hypoxic response. HIF was discovered and first mentioned as the transcriptional regulator of the erythropoietin gene (EPO) in renal fibroblasts and HIF activation under low oxygen concentrations was found to lead to an increased EPO production [80]. There are three genes that encode α-subunits of HIF in mammals (HIF-1α, HIF-2α and HIF-3α). HIF-1 consists of two subunits, α (inducible) and β (constitutively-expressed, or ARNT).

In the presence of oxygen, proline residues in the oxygen-dependent degradation domain of HIF-1α are hydroxylated by prolyl hydroxylases (PHDs) [81]. This enables the von Hippel-Lindau (VHL) protein to recognize HIF-1α, causing it to be ubiquitylated and targeted to the proteasome for degradation [82]. The process is

precisely regulated in several ways, including cofactor dependencies of the PHDs such as ascorbate (Vitamin C), Krebs cycle intermediates, and iron [83].

In oxygen-deprived tissues (below 2% O_2), HIF α-subunits become stabilized and consequently activated due to the diminished activity of the prolyl hydroxylases (PHDs) and hetero-dimerize with ARNT. These heterodimers recognize and bind to hypoxia response elements (HRE) (5'-[AG]CGTG-3'), specific genomic sequences that lie within target gene promoters and recruit transcriptional co-activators such as p300/CBP for full transcriptional activity (Figure 7). This leads to changes in the transcription of genes that are necessary to overcome oxygen deprivation [80]. HIF-1α activation helps cells to adapt to oxygen deprivation by regulating the expression of genes involved in proliferation, metabolism, angiogenesis and invasion/metastasis [84].

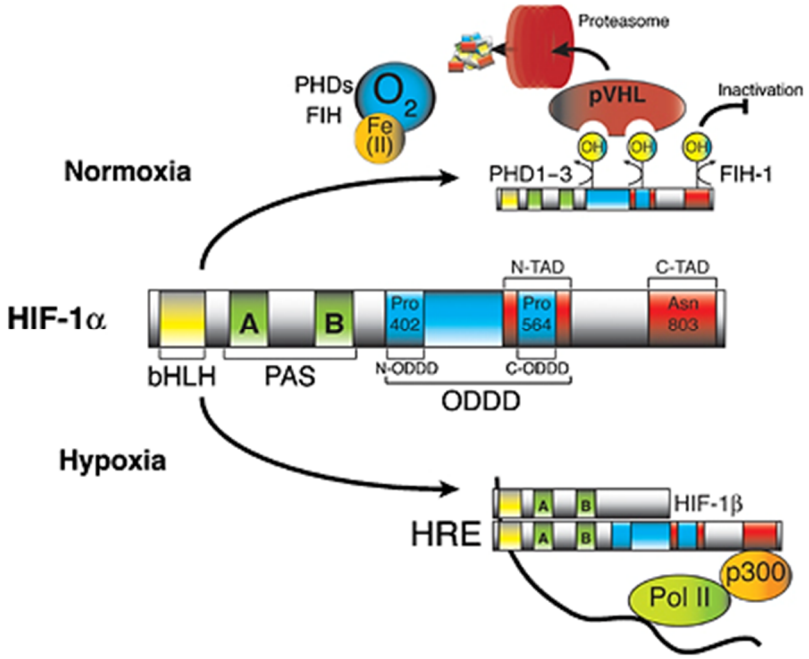

Figure 7 - HIF-1α structure and its regulation.

The HIF-1α cascade and its fate under normoxic and hypoxic conditions. The Figure was adapted from Weidemann et al., 2008 [82].

Historically, most research has been centered around HIF-1α, but more recently specific targets and roles of HIF-2α have become well understood. Hypoxia inducible transcription factor 2α (HIF-2α) is a protein with sequence similarity to HIF-1α, also regulated by proline hydroxylation. HIF- 2α activates transcription of a group of target genes that overlap with, but are distinct from those regulated by HIF-1α [85], [86]. For

example, opposing effects of HIF-1α and HIF-2α on the activity of c-Myc have been reported [87]. Furthermore, there is evidence that HIF-1α is more important for metabolic regulation in cancer cells, while HIF-2α is thought to mainly act on the regulation of angiogenic and metastatic processes [88]. In contrast to the presented transcription factors, the HIF-3α is an inhibitor of HIF-1α that is rarely studied and is thought to be involved in feedback regulation [89].

The activity of HIF-1α is controlled on several levels and various studies have shown elevated levels of HIF-1α and/or HIF-2α in primary tumors and their metastases [90], [91]. Oncogenic pathways can stabilize HIF-1α, of which the best described are the RAS and the PI3K/Akt pathways [92]. Additionally, growth factors such as HER2, especially when upregulated, can also increase HIF-1α synthesis, primarily via the action of mammalian target of rapamycin (mTOR). The balance of these pathways is critical for tumor growth and development [93]. Furthermore, fluctuations in hypoxia typically seen in tumors, has been shown to generate a higher level of stabilized HIF-1α than a stable hypoxia exposure [94]. HIF-1α activates multiple hypoxia-response genes with roles in many aspects of cancer biology, including angiogenesis, immune evasion, pH regulation, glycolysis, invasion and metastasis [95], [96], [97], [98], [99]. Thus, HIF-1α induces a number of genes which enable cells to adapt to low oxygen condition, and thereby contribute to cancer progression. The elevation of HIF-1α and HIF-2α expression levels is associated with increased tumor growth and poor prognosis in the majority of human tumors including breast cancer [100].

1.4.3 Limitations of existing hypoxia markers

Tumor cells exhibit a distinct growth pattern into surrounding healthy tissue accompanied by limited access to the vascular system for certain areas of the tumor. This also leads to heterogenic features in hypoxic regions. These hypoxic regions correlate with increased HIF-1α and HIF-2α levels and have been associated with a poor OS signature in several cancers like brain, pancreas, colon and breast [101].

Assessing hypoxia in tumors is a complicated matter since current methods have significant limitations. Measuring pO_2 directly via polarographic needle electrodes is invasive and provides no information about the hypoxic distribution across the whole tumor architecture [102]. Nuclear medicine imaging and radiological techniques can provide suitable data but are expensive, suffer from low resolution and are hard to

standardize between many centers. In addition, the markers used are mainly dependent on the glycolytic state of the cell [103].

Another way to assess hypoxia may be through the expression of many hypoxia-induced genes, like the median RNA expression signature of a 99-gene set predicting recurrence-free survival in head and neck cancer [104]. Similarly, a gene-expression signature of the cellular response to hypoxia was developed for prognosis in ovarian and breast cancer [105].

Therapeutic drugs in the hypoxic context, like Bevacizumab, a monoclonal antibody targeting VEGFA, have shown some promising effects in certain cancers such as renal cancer and metastatic colorectal cancer. However, in other entities such as breast cancer the patient benefits were rather disappointing. It has been demonstrated that hypoxic breast tumors do no respond well to established therapeutics and predominantly show poorer clinical outcome [106]. Identifying novel targets within these hypoxic tumors is a necessary need and a worthwhile endeavor.

Along this line, most studies lack novelty and translation into the proteomic level. Therefore, a part of my PhD project aimed to address this issue and to investigate a new hallmark of cancer in the context of hypoxia at a proteomic level via reverse phase protein arrays.

1.5 Reverse phase protein arrays

1.5.1 The RPPA technology

The Reverse Phase Protein Array (RPPA) technology represents a highly efficient and cost effective successor of miniaturized immunoassays that use a sandwich format for antigen capture [107], [108]. First described by Paweletz et al. in 2001, the term "reverse phase" refers to the analytes (antigen) which are immobilized on a solid phase (nitrocellulose), and subsequently probed with an antibody against a specific target [109]. RPPA allows to multiplex quantitative measurements of total, phosphorylated, glycosylated, acetylated or cleaved proteins from multiple samples [110]. The technology is widely used for protein expression profiling and signal pathway mapping in cell lines, clinical specimen, as well as serum and plasma samples [111], [112], [113], [114]. The basic readout is usually reflected in the detection of a unique change in expression of one protein, or pattern of changes in many proteins as well as protein networks (Figure 8).

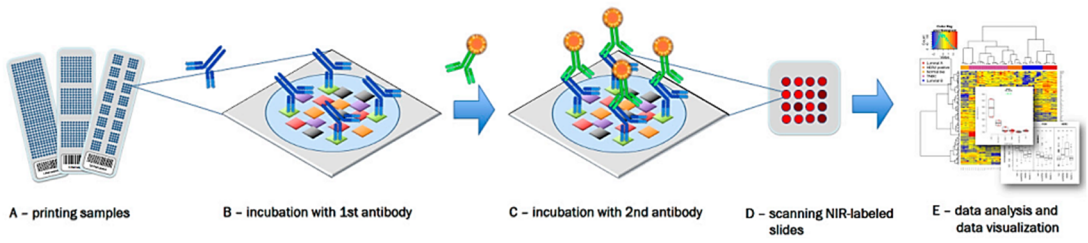

Figure 8 - The basic principle of RPPA.

Reverse phase protein arrays (RPPA) experimentation involves (A) printing of samples in a neatly organized array format onto, for example, nitrocellulose-coated glass slides; (B) Incubation with a highly target-specific primary antibody to detect proteins-of-interest, or a certain phosphorylation sites; (C) Signal detection of the primary antibody is commonly performed by fluorescence, chemiluminescence or colorimetric methods; (D) Target intensities are quantified after scanning and analyzing signal intensities of individual spots; (E) Data processing and quality control. NIR, Near-infrared.

During the last decade, the RPPA approach has been used for several applications in the field of system biology and biomarker discovery in different tumor entities [115], [116]. RPPA has been shown to be able to concurrently measure a large number of

analytes with an analytical precision and accuracy similar or superior to clinical-grade assays such as ELISAs [114]. Especially the high throughput capabilities and sensitivity of RPPA paved the way for in depth investigations of tissue samples, usually originating from small-bore core biopsies or fine needle aspirates, with exceedingly small amounts of target material. Unlike other existing competing technologies, RPPA can quantitatively measure large numbers of low abundance analytes, such as phosphorylated signaling proteins, from a single small sample input [117]. Several studies could show, that this technology can generate linear quantitative data with an analytical sensitivity of detection in the fg/ml range with linearity in the sub pg/ml range, which is several orders of magnitude more sensitive compared to current multiple reaction monitoring (MRM) mass spectrometry approaches [118], [119], [120]. In addition, the throughput of RPPA is currently not feasible by conventional western blot or any other proteomic technology.

Taken together, RPPA represents a rapidly emerging and advancing cost-effective technology that is able to quantitatively analyze hundreds of proteins and post-translational modifications in small samples sizes. While other proteomic approaches like mass spectroscopy hold great promise for the analysis of samples, they do not currently have the throughput, sensitivity and ability to deal with small amounts of material, or the cost effectiveness of the RPPA platform [121].

1.5.2 RPPA platform at DKFZ

The RPPA platform at the Division of Molecular Genome Analysis (DKFZ) was established in 2007 and further developed in terms of automation and data processing in the recent years [122], [123], [124]. The general principle of the RPPA platform at DKFZ is outlined in Figure 9 and a detailed workflow description can be found in Chapter 3, Section 3.2.7. The flexibility of the RPPA technology to analyze large sample numbers in parallel either in an unbiased approach or for a protein network of choice, remains the major strength of the platform and provides the opportunity to study hundreds of patient samples simultaneously. Based on these core attributes that favor biomarker guided clinical research and the ability to identify therapeutic markers that could be suitable for patient stratification, I used the RPPA platform as the method of choice for my PhD project.

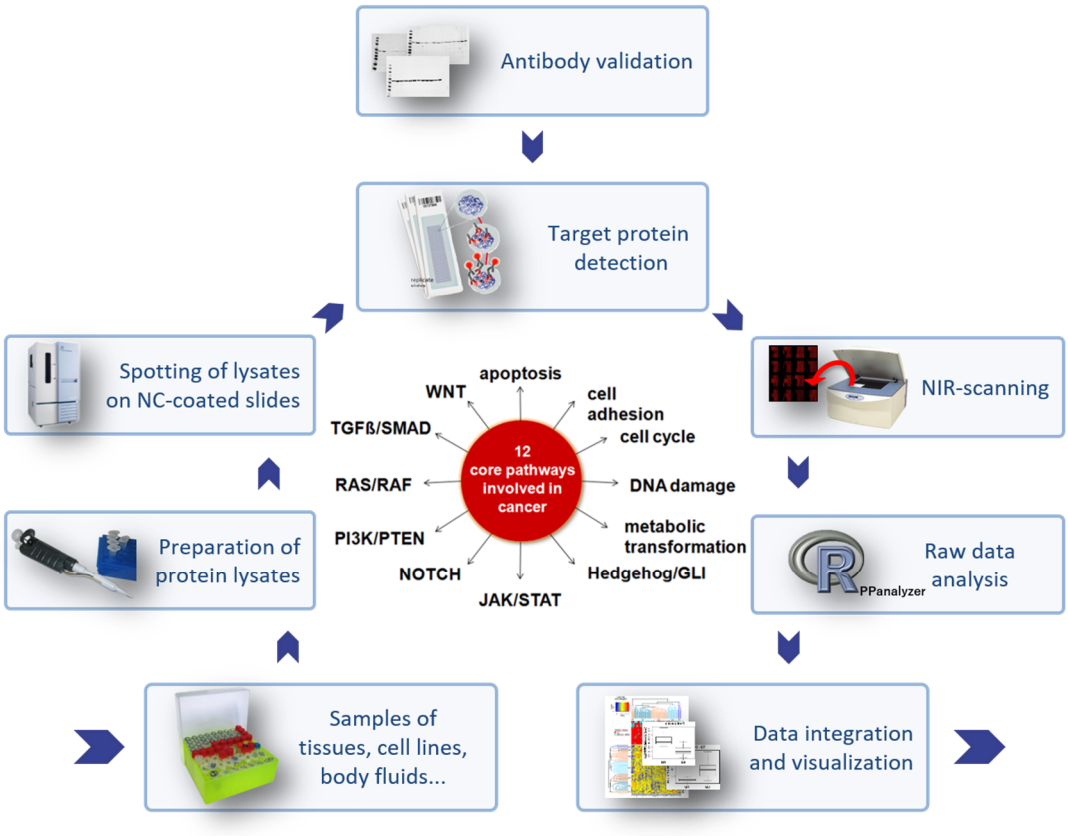

Figure 9 - RPPA workflow at DKFZ.

Schematic presentation of the DKFZ workflow of using reverse phase protein arrays for a targeted profiling. NC, Nitrocellulose; NIR, Near-infrared.

The reliability of RPPA highly depends on the quality of the antibodies used. However, universally applied guidelines or a standardized workflow for determining the antibodies applicable for use in RPPA has not yet been established. Antibody validation during my PhD was carried out as previously described [125]. Primary antibodies were selected in order to cover a range of metabolic pathways and to achieve a broad perspective on breast cancer metabolism. Please refer to Chapter 3, Section 3.1.5 for further information on antibodies relevant to this project.

Chapter 2

Aims of the project

Breast cancer tumors are highly heterogeneous and differences in their metabolic phenotypes are not well understood. While a number of mostly RNA-based profiling studies have aimed at improving diagnosis and therapy decision, few tests have entered clinical practice. Furthermore, less is known about the metabolic phenotype of breast cancer, especially on a proteomic scale. Currently there are no studies that have systematically examined the prognostic value of metabolism associated enzymes in a large cohort of breast cancer patients or investigated the dynamic behavior of microenvironmental factors like hypoxia on cancer metabolism in a time resolved manner.

In order to provide novel insides into the proteomic landscape of breast cancer, I addressed the following questions:

Is a targeted proteomic approach applicable towards the characterization of breast tumors at the metabolic level?

- A large cohort of breast tumor specimen was utilized via targeted proteomics and further statistically examined for metabolic features.

Which metabolic enzymes, transporters and regulators are important for the survival of breast cancer patients and could serve as potential biomarkers?

- Based on the generated protein expression matrix, the relationship between metabolism-associated protein expression profiles and clinicopathological characteristics were evaluated.

What are the metabolic adaptive responses under hypoxia and its main regulators?

- Time resolved breast cancer cell line data was generated via targeted proteomics and further processed by bioinformatic methods. Findings were assessed in order to reveal metabolic changes, with a focus on top regulated targets.

Chapter 3

Materials and Methods

3.1 Materials

3.1.1 Patient cohort and clinical samples

Human primary breast cancer samples were collected at the Martin-Luther University, Halle-Wittenberg between 2009 and 2011 as part of the multicenter prospective PiA trial (NCT 01592825). Only fresh frozen tissue samples of female patients with operable non-metastasized breast cancer were included. The study was approved by the ethics committee of the Martin-Luther University Halle-Wittenberg and informed consent had been obtained from each patient. I investigated a cohort of 801 primary tumor tissue samples with RPPA. Tumor specimens were fresh frozen after surgery and stored at −80 °C until further use. Tumor content was verified by histopathology. Clinicopathological parameters were obtained for each patient and documented using SPSS 22. TNM staging system was used [126]. Patient information was anonymized prior to analysis. Receptor defined breast cancer subtypes were determined according to the St. Gallen classification [12]. Due to missing Ki-67 values, histopathological grading was used to assess cell proliferation [127]. The standardized definitions for efficacy end points (STEEP) criteria were used as endpoint definitions [128].

The following stratification system was applied:

Luminal A-like:	Estrogen receptor (ER) positive and/or Progesterone receptor (PgR) positive, HER2 negative, grade 1 or 2.
Luminal B-like: (HER2 negative)	ER positive and/or PgR positive, HER2 negative, grade 3.
Luminal B-like: (HER2 positive)	ER positive and/or PgR positive, HER2 positive, all grades.
HER2 positive: (non-luminal-like)	ER negative and PgR negative, HER2 positive, all grades.
Triple negative: (TNBC)	ER negative, PgR negative, HER2 negative, all grades.

3.1.2 Instruments

Aushon 2470 contact printer	Aushon BioSystems (Billerica, US)
BINDER Cell culture incubator	BINDER GmbH (Tuttlingen, DE)
Biofuge fresco centrifuge	Heraeus (Hanau, DE)
Biohit Proline multichannel pipette	Sartorius (Göttingen, DE)
BP121S and BP2100S balances	Sartorius (Göttingen, DE)
CASY cell counter	Roche Innovatis AG (Bielefeld, DE)
Dri-block®DB-2D heating block	Bibby Scientific Limited (Stone, UK)
DURAN® desiccator	Schott (Mainz, DE)
ErgoOne® pipette	Starlab International (Hamburg, DE)
HERA Safe cell culture hood	Thermo Fisher Scientific (Waltham, US)
Infinite M200 microplate reader	Tecan Group (Männedorf, CH)
inoLab pH meter	WTW (Weilheim, DE)
Liebherr Premium Freezer	Liebherr-International (Biberach an der Riß, DE)
Liebherr Premium Fridge	Liebherr-International (Biberach an der Riß, DE)
Milli-Q Biocel purification system	Merck Millipore (Darmstadt, DE)
Mini-Protean®II electrophoresis cell system	BioRad (München, DE)
Microscope IXM XL	Molecular Devices (Sunnyvale, US)
MR3001 magnetic stirrer	Heidolph (Schwabach, DE)
Multipette®plus hand-held dispenser	Eppendorf AG (Hamburg, DE)
Odyssey® Infrared Imaging System	LI-COR Biosciences (Lincoln, US)
Pipetboy acu pipette	INTEGRA Biosciences (Fernwald, DE)
Pipetman® pipette	Gilson (Limburg, DE)
Thermomixer comfort	Eppendorf AG (Hamburg, DE)
TissueLyser bead mill	Qiagen (Hilden, DE)
Titramax 100 rocking platform	Heidolph (Schwabach, DE)
Trans-Blot® Turbo™ Transfer System	BioRad (München, DE)
Tube Rotator	VWR (Darmstadt, DE)
Vacuboy aspiration device	INTEGRA Biosciences (Fernwald, DE)
VortexMixer 7-2020	neoLab (Heidelberg, DE)

3.1.3 Consumables

348-well plate, AB-1056	Abgene (Epsom, UK)
1.5 mL micro centrifuge tube	Eppendorf AG (Hamburg, DE)
10cm Ø Petri dish	Techno Plastic Products (TPP) AG (Trasadingen, CH)
15mL conical tube	Becton Dickinson (New Jersey, US)
2 mL micro centrifuge tube	Eppendorf AG (Hamburg, DE)
50mL conical tube	Becton Dickinson (New Jersey, US)
6-well plate	Nunc, Thermo Fisher Scientific (Waltham, US)
96-well plate	Becton Dickinson (New Jersey, US)
Adhesive Optically Clear Plate Seal	Thermo Fisher Scientific (Waltham, US)
Anaeroclip®	Merck KGaA (Darmstadt, DE)
Anaerotest®	Merck KGaA (Darmstadt, DE)
Casy cup	Roche Innovatis AG (Bielefeld, DE)
Cell Culture Flasks, T-25, T-75, T-175	Greiner Bio-One International GmbH (Kremsmünster, AT)
Cell Scraper	Corning (Corning, US)
Combitip	Eppendorf AG (Hamburg, DE)
Cry vials 1.8mL	Nunc, Thermo Fisher Scientific (Waltham, US)
Desiccant bag	Conrad Electronics (Hirschau, DE)
Filter tips, 10µL, 20µL, 100µL, 200µL, 1000µL	Neptune Scientific (San Diego, US)
Mini-PROTEAN® TGX™ Precast Gel	BioRad (München, DE)
Oncyte® Avid Nitrocellulose Film-Slide	Grace Bio-Labs (Bend, US)
pipette tip	Becton Dickinson (Heidelberg, DE)
Scalpel Feather No21	pfm medical (Köln, DE)
Serological pipettes 2.5mL, 5mL, 10mL, 25mL, 50ml	Becton Dickinson (New Jersey, US)
Stainless steel bead (5 mm)	Qiagen (Hilden, DE)
Trans-Blot® Turbo™ LF PVDF membrane	BioRad (München, DE)
Trans-Blot® Turbo™ Transfer Stacks	BioRad (München, DE)
Whatman paper	GE Healthcare (München, DE)

3.1.4 Chemicals and reagents

CASYton	Roche Innovatis AG (Bielefeld, DE)
cOmplete Mini Protease Inhibitor Cocktail	Roche Diagnostics (Mannheim, DE)
EDTA	Sigma-Aldrich (Saint-Louis, US)
Ethanol	Sigma-Aldrich (Saint-Louis, US)
Fast Green FCF	Carl Roth (Karlsruhe, DE)
KCL	Sigma-Aldrich (Saint-Louis, US)
Methanol	Greiner Bio-One International GmbH (Kremsmünster, AT)
M-PER mammalian protein extraction reagent	Thermo Fischer Scientific (Rockford, US)
NaCl	VWR International (Darmstadt, DE)
NaOH	Sigma-Aldrich (Saint-Louis, US)
peqGOLD Protein Marker IV and V	PEQLAB Biotechnologie (Erlangen, DE)
PhosSTOP Phosphatase Inhibitor Cocktail	Roche Diagnostics (Mannheim, DE)
Rockland Blocking Buffer	Rockland Immunochemicals Inc. (Limerick, US)
Roti®-Load 1, 4x sample loading buffer	Carl Roth (Karlsruhe, DE)
Staurosporine	Merck Millipore (Darmstadt, DE)
SDS	Carl Roth (Karlsruhe, DE)
Trans-Blot® Turbo™ Transfer Buffer	BioRad (München, DE)
Tris HCl	Sigma-Aldrich (Saint-Louis, US)
Tris-base	Sigma-Aldrich (Saint-Louis, US)
Triton X-100	Sigma-Aldrich (Saint-Louis, US)
Tween 20	Sigma-Aldrich (Saint-Louis, US)

3.1.5 Antibodies

Primary Antibodies

Dataset ID	Gene ID	Catalog#	Company
ACC	ACACA	3662	Cell Signaling Technology (US)

Dataset ID	Gene ID	Catalog#	Company
ACC_Ser79	ACACA	3661	Cell Signaling Technology (US)
ARG2	ARG2	GTX118048	GeneTex (US)
ASCT2	SLC1A5	8057	Cell Signaling Technology (US)
ASL	ASL	HPA016646	Sigma-Aldrich (US)
ASS1	ASS1	HPA020896	Sigma-Aldrich (US)
CAD	CAD	11933	Cell Signaling Technology (US)
CPS1	CPS1	ab128942	Abcam plc (UK)
ER alpha	ER	E1678C002	DCS (DE)
FASN	FASN	ab128856	Abcam plc (UK)
FH	FH	sc100743	Santa Cruz Biotechnology (US)
GAPDH	GAPDH	GTX 627408	GeneTex (US)
GLK	GCK	GTX111517	GeneTex (US)
GLS	GLS	ab156876	Abcam plc (UK)
Glud12	GLUD	12793	Cell Signaling Technology (US)
GLUL	GLUL	WH0002752M1	Sigma-Aldrich (US)
GLUT1	SLC2A1	ab115730	Abcam plc (UK)
GLUT4	SLC2A4	2213	Cell Signaling Technology (US)
GOT1	GOT1	ab170950	Abcam plc (UK)
GPT2	GPT2	sc398383	Santa Cruz Biotechnology (US)
HER2	ERBB2	AB17MS730	Thermo Fisher Scientific (US)
Hif1_alpha	HIF1A	10006421	Cayman Chemical (US)
Hif2_alpha	HIF2A	7096	Cell Signaling Technology (US)
IDH1	IDH1	8137	Cell Signaling Technology (US)
IDH2	IDH2	12652	Cell Signaling Technology (US)
Ki67	MKI67	M7240	Dako (US)
LAT1	SLC7A5	5347	Cell Signaling Technology (US)
LDHA	LDHA	3582	Cell Signaling Technology (US)
LDHB	LDHB	MAB2732	Abnova (TW)
NAGS	NAGS	AV51183	Sigma-Aldrich Co. (US)
ODC1	ODC1	ab126590	Abcam plc (UK)
PCK1	PCK1	12940	Cell Signaling Technology (US)
PCK2	PCK2	sc32879	Santa Cruz Biotechnology (US)
PDH	PDHA1	3205	Cell Signaling Technology (US)
PGR	PGR	1483	Epitomics (US)
PHGDH	PHGDH	13428	Cell Signaling Technology (US)
PKM1	PKM1	7067	Cell Signaling Technology (US)

Dataset ID	Gene ID	Catalog#	Company
PKM2	PKM2	4053	Cell Signaling Technology (US)
PSAT1	PSAT1	GTX110576	GeneTex (US)
PSPH	PSPH	HPA020376	Sigma-Aldrich Co. (US)
SDHA	SDHA	sc59687	Santa Cruz Biotechnology (US)
SHMT2	SHMT2	HPA020543	Sigma-Aldrich Co. (US)
SLC14A1	SLC14A1	ab67595	Abcam plc (UK)
SMS	SMS	GTX114783	GeneTex (US)
SREBP1	SREBF1	NB100-74542	Novus Biologicals, Inc. (US)
STARD10	STARD10	HPA026661	Sigma-Aldrich Co. (US)

Secondary Antibodies

Format	Reactivity	Conjugate	Company
full-length IgG	rabbit IgG (H+L)	Alexa Flour® 680	Life Technologies (US)
full-length IgG	mouse IgG (H+L)	Alexa Flour® 680	Life Technologies (US)
F(ab')2	rabbit IgG (H+L)	Alexa Flour® 680	Life Technologies (US)
F(ab')2	mouse IgG (H+L)	Alexa Flour® 680	Life Technologies (US)

3.1.6 Buffers and solutions

10x TBS:	1.37 M NaCl 200 mM Tris pH 7.6
10x TBST:	0.1% Tween20® in 10x TBS
Cell line lysis buffer:	mammalian protein extraction reagent (M-PER) 1 tablet PhosSTOP Phosphatase Inhibitor Cocktail 1 tablet Complete Mini Protease Inhibitor Cocktail
Tissue lysis buffer:	50 mM Tris, pH 8.5 138 mM NaCl 2.7 mM KCl 1% Triton X-100
SDS-PAGE running buffer:	192 mM glycine 25 mM Tris 0.1% SDS

Transfer buffer 1L:	20% Trans-Blot® Turbo™ 5x Transfer Buffer 20% EtOH 60% H_2O
Blocking buffer:	50% Rockland blocking buffer 5 mM NaF 1 mM Na_3VO_4 ad TBS
Washing buffer:	0.1% Tween®20 in TBS (TBST)
4x RPPA printing buffer:	10% Glycerol 4% SDS 10 mM DTT 125 mM Tris pH 6.8
FCF staining solution:	0.005% Fast Green FCF 10% acetic acid 30% ethanol
FCF destaining solution:	10% acetic acid 30% ethanol

3.1.7 Kits

Pierce™ BCA Protein Assay Kit	Thermo Fisher Scientific (Waltham, US)
Anaerocult® A mini	Merck KGaA (Darmstadt, DE)
Trans-Blot® Turbo™ RTA Transfer Kit	BioRad (München, DE)

3.1.8 Cell culture

Breast cancer cell lines were purchased from the American Type Culture Collection ATCC (LGC Standards GmbH, Wesel, DE). Cell line authentication was performed via multiplex cell line authentication (Multiplexion GmbH, Friedrichshafen, DE).

Cell line	Characteristics
MCF-7	ER+, HER2-, epithelial-like, adenocarcinoma from pleural effusion
SKBR3	ER-, HER2+ (amplified), epithelial-like, adenocarcinoma from pleural effusion
MDA-MB-231	ER-, HER2-, epithelial-like adenocarcinoma from pleural effusion

MDA-MB-468	ER-, HER2-, epithelial-like, adenocarcinoma from pleural effusion

Media and reagents used for cell culture

0.25% Trypsin EDTA (1x)	Gibco BRL (New York, US)
Fetal Bovine Serum	Gibco BRL (New York, US)
RPMI 1640 (+ L-Glutamine)	Gibco BRL (New York, US)
RPMI 1640 (- L-Glutamine)	Gibco BRL (New York, US)
Dulbecco's Phosphate Buffered Saline	Gibco BRL (New York, US)

3.1.9 Software

GenePix Pro 7.0	Molecular Devices (Sunnyvale, US)
GraphPad Prism 5	GraphPad Software Inc. (La Jolla, US)
Molecular Devices MetaXpress	Molecular Devices (Sunnyvale, US)
Odyssey 3.1	LI-COR Biosciences (Lincoln, US)
R version 3.0.2	R Development Core Team (www.R-project.org)
SPSS 22	SPSS Inc. (Illinois, US)

3.2 Methods

3.2.1 Preparation of protein extracts from cell lines

Cells were lysed on ice with pre-chilled cell line lysis buffer (M-PER lysis buffer containing protease inhibitor Complete Mini and anti-phosphatase PhosSTOP). Cell lysates were incubated on a tube rotator for 30 min at 4°C and subsequently centrifuged for 10 min at 16.000 x g. Supernatant was stored at -80°C until further use. Total protein concentration was quantified with Pierce™ BCA Protein Assay Kit according to manufacturer's instructions.

3.2.2 Preparation of protein extracts from tumor samples

Frozen tumor specimens were homogenized using a bead mill and pre-chilled tissue protein extraction reagent (50 mM Tris, pH 8.5, 138 mM NaCl, 2.7 mM KCl, 1% Triton X-100). Tumor lysates were centrifuged at 16.000 x g for 10 min at 4°C. The homogenized tumor lysate supernatants were aliquoted and stored at -80°C until further use. Total protein concentration was quantified with Pierce™ BCA Protein Assay Kit according to manufacturer's instructions.

3.2.3 Immunoblotting

Protein lysates were denatured using 4x sample loading buffer (Roti®-Load 1) for 5min at 95°C. Samples were loaded on Mini-PROTEAN® TGX™ Precast Gels for protein mass separation and a prestained protein ladder (peqGOLD Protein Marker IV and V) was used as molecular mass marker. After protein separation via SDS-PAGE, the proteins were transferred to a polyvinylidene difluoride membrane (Trans-Blot® Turbo™ LF PVDF membrane) by electrophoresis. The Trans-Blot® Turbo™ Transfer System was used for the "semi dry" blotting set-up in accordance to the manufacture instructions. Afterwards the membrane was blocked for 1h at RT with blocking buffer and subsequently incubated with target specific primary antibody over night at 4°C on a rocking platform. The membrane was washed 4 x 5 min in TBST followed by an 1h incubation with Alexa Flour® 680 conjugated secondary antibody. After washing for 4 x 5 min, the membrane was scanned at an excitation wavelength of 685 nm and a

resolution of 84 µm using the Odyssey® Infrared Imaging System. For western blot quantification, local background subtraction and β-Actin normalization was performed.

3.2.4 Antibody validation

Each antibody was tested for specificity to assure the detected signal is representative for the target of interest. The gold standard for antibody validation is western blot. A pool of different breast cancer cell lines was used as test samples. All antibodies resulting in a target specific single band or characteristic band pattern were used for RPPA. Antibodies resulting in several unspecific bands were not used for RPPA. All Antibodies used for RPPA profiling are provided in Chapter 3, Section 3.1.5.

3.2.5 Immunohistochemistry

Immunohistochemistry (IHC) analyses were performed by PD Dr. med. Jörg Buchmann at the pathology department of the Martin-Luther University Halle-Wittenberg on 4-micron tissue sections. Protein expression was assessed using Bond Max Polymer Refine Immunohistochemistry protocol. Primary SHMT2 and ASCT2 antibody was diluted 1:250. Epitope retrieval was performed with Bond Epitope Retrieval Solution for 30 minutes at pH6, followed by a peroxidase block. Primary antibody was incubated for 20 minutes and detected using Bond Polymer Refine Detection with DAB substrate. IHC were assessed by a pathologist as a visual score, semi-quantitative based on the fraction of cytoplasmic staining above background.

3.2.6 Hypoxia exposure

Exposure of cell cultures to hypoxia (1,2% or 0.2% oxygen) was undertaken in a cell culture incubator at 1.2% oxygen or in hypoxia bags at 0.2% oxygen (Anaerocult® A mini). In parallel, cells were maintained in normoxic conditions (5% CO_2, 37°C, 21% oxygen). All experiments were performed in triplicate from independent cell cultures.

3.2.7 Reverse phase protein arrays

Tumor and cell line lysates were adjusted to a total protein concentration of 2 µg/µl. Samples were mixed with 4 x RPPA printing buffer (10% glycerol, 4% SDS, 10 mM DTT, 125 mM Tris–HCl, pH 6.8) and denatured at 95°C for 5 min. Protein lysates were transferred to 348-well plates and centrifuged for 2 min at 200 x g. Six step dilution series of tumor samples/cell line pools were serving as internal controls. All samples were printed as technical triplicates on Oncyte® Avid Nitrocellulose Film-Slides using a Aushon 2470 contact printer equipped with 185 µm solid pins (1.6 nl sample per spot, average spot diameter 250 µm). The humidity during the printing run was kept constant at 80%. Slides were stored after the print run at -20°C with desiccant. Post spotting, slides were incubated with blocking buffer in TBS (50%, v / v) containing 5 mM NaF and 1 mM Na3VO4 for 2h at room temperature. Each array was subsequently incubated with target-specific primary antibodies at 4°C overnight. Representative subarrays were incubated without primary antibody and served as "blank" control. After performing washing steps with 4 x 5 min TBST the detection of primary antibodies was carried out with Alexa Fluor® 680 F(ab')2 fragments of goat anti-mouse IgG or anti-rabbit IgG in 1:12000 dilution for 1h at RT. Slides were washed 4 x 5 min with TBST followed by two final washing steps with ultra-pure water for 5 min. Slides were air dried and further utilized in the imaging process. All incubation and washing steps were performed on a rocking platform and slides were protected from light. Every ninth slide of each run was stained using Fast Green FCF protein dye for total protein quantification and served as normalization reference. TIFF images (16 bit) of all slides were obtained at an excitation wavelength of 685 nm and a resolution of 21 µm using the Odyssey® Infrared Imaging System.

Signal intensities of individual spots were quantified using GenePixPro 7.0 software. The aquirred TIFF image of each slide and gene pix array list file, generated by the printer to map the sample location on the slide, were matched into a gene pix result file. At this step, a visual inspection of each spot was performed and slides without uniform background signal were excluded from further analysis. RPPA raw data preprocessing and quality control were performed using the *RPPanalyzer* R-package [123]. The gene pix result files as well as sample and antibody information text files were required for further raw data analysis. The raw signal intensities of the control samples were plotted against the respective total protein concentration. Only data of

antibodies showing a linear correlation between target signal intensity and protein concentration were used for further analysis. Next, target signals were normalized to the total protein amount per spot via Fast Green FCF control. After median calculation of technical replicates, normalized target signal intensities were plotted against the signal intensities obtained by incubation of primary antibody controls (blank signal). Normalized protein data was saved in text files and further explored in collaboration with our collaboration partners at the Department of Medical Statistics at University Medical Center Goettingen (Goettingen, Germany) and the Institute of Physics at the Freiburg Institute for Advanced Studies (Freiburg, Germany).

3.2.8 Statistical and bioinformatic analyses

If not stated otherwise, the data was analyzed using GraphPad Prism 5 or the R statistical computing environment (version 3.0.2) [129]. A p value < 0.05 was considered statistically significant.

STRING visualization

STRING Database (Version 10) of the STRING Consortium was used for visualization of protein interactions by choosing Gene IDs corresponding to proteins [130].

Hierarchical clustering

Hierarchical cluster analysis was performed on z-scores of protein expression levels using Ward's minimum variance method and squared euclidean distance. Patient samples and protein targets were clustered simultaneously and the resulting dendrograms were visualized together with a heatmap depicting z-score values. *RPPanalyzer* R-package was used for visualization, with an adjustment of color bars according to the clinicopathological features of interest and exploiting the *dendextend* R-package for dendrogram color-coding [123], [131].

Univariate analysis

The relationship between clinicopathological variables and the three patient clusters was evaluated using analysis of variance (ANOVA), Kruskal-Wallis rank sum test,

and Fisher's Exact test, as appropriate. The relationship between the variables and the patient groups, stratified based on the median expression of a protein, was evaluated using t-test, Wilcoxon rank sum test, and Fisher's Exact test, as appropriate.

Multivariate and survival analysis

Patients stratified into groups (based on receptor-defined subtypes, median expression level or patient dendrogram clusters) were subjected to Kaplan-Meier analysis of overall survival (OS) and recurrence-free survival (RFS). The difference of Kaplan-Meier curves was tested using the log-rank test implemented in the *survival* R-package [132]. Univariate Cox proportional hazard regression models were applied to test individual protein target association with OS and RFS [133]. For each target, the exponent of the estimated regression coefficient is reported as a hazard ratio (HR) along with its 95% confidence intervals (CI). P values were adjusted for multiple testing resulting in false-discovery rate (FDR) values [134]. Univariate Cox proportional hazard regression models were further used to evaluate clinicopathological variables. Multivariate Cox analyses were then performed on selected non-correlated clinicopathological covariates for each of the proteins that showed significance in the univariate Cox analysis. The median follow-up time of the cohort was 55.44 months for OS and 54.46 months for RFS.

Linear regression model

The preprocessed data of the time courses with triple replicates for each time point were analyzed individually for each target protein and for each of the 12 combinations of cell lines and treatments. In order to merge the replicates and asses the kind and strength of regulation, a linear regression model was used for the log2(10) signal intensities of the target protein time courses and cell line-treatment combination individually. The Cook's distance was used to detect outliers in the measured time course [135] [136]. Based on this, 1% of data points was removed from the further analysis. A one-way analysis of variance (ANOVA) was applied to each time course in order to discriminate between a constant time course signal at the basal expression level of the target protein and significantly regulated expression profiles ($pANOVA < 0.05$). Using t-statistics, time point specific regulation estimates have been tested

individually against the respective basal expression estimate in order to identify significantly regulated signals ($p < 0.05$). P-values are FDR adjusted for multiple testing using the Benjamini-Hochberg procedure.

TCGA data analysis

Analyses of The Cancer Genome Atlas (TCGA) data was conducted on primary breast cancer tumor samples with both RNA-sequencing data and clinical annotations. Level 3 normalized gene expression data (TCGA_BRCA_exp_HiSeqV2-2015-02-24) was obtained from the cBioPortal website [137], [138]. Gene expression data was log2 transformed and subset to the genes of interest.

Chapter 4

Results

4.1 Proteomic profiling of cancer metabolism in breast cancer patients

4.1.1 RPPA patient dataset generation

In order to investigate altered expression patterns of metabolism related proteins in the tumorigenesis of breast cancer, I established a collaboration with the gynecology department of the university clinic at the Martin-Luther-University Halle-Wittenberg (Halle(Saale), DE). With the aim to generate a proteomic dataset of breast cancer specimens, Dr. Eva Kantelhardt and Dr. Martina Vetter kindly provided me with over 800 breast cancer samples of patients, diagnosed with primary breast carcinoma, for my research. The specimens received are part of an ongoing clinical trial and further information on clinicopathological features of the cohort are summarized in Table 2 and in Chapter 3, Section 3.1.1.

In a first step, the tumor specimens were lysed as described in Chapter 3, Section 3.2.2 and I further determined the protein concentration of each sample. Afterwards I processed the samples via reverse phase protein arrays and produced protein array slides primed for primary antibody incubation. 37 suitable protein targets with relevance to cancer metabolism were chosen and conscientious antibody validation was performed. The RPPA slides were then incubated with the validated antibodies and a quantitative analysis of protein expression was performed. The RPPA protocol is reported in Chapter 3, Section 3.2.7. After quality control of the raw RPPA data from my side, the data matrix was further explored in collaboration with Dr. Astrid Wachter and Dr. Michaela Bayerlová of the Department of Medical Statistics, University Medical Center Goettingen (Goettingen, DE). The whole RPPA data matrix matched with clinical data is provided in the Appendix (Table S5).

Table 2 - Patient and tumor characteristics

	Total	(%)
Number of patient samples		
Total	801	(100)
Age		
Mean ± SD	62.25 ± 13.7	
Median (range)	63 (22-90)	
Tumor size		
< 2cm	400	(49.9)
≥ 2-5cm	358	(44.7)
> 5cm	43	(5.4)
Histology		
Ductal	638	(79.7)
Lobular	118	(14.7)
Other	45	(5.6)
T stage		
T1	413	(51.6)
T2	342	(42.7)
T3	38	(4.7)
T4	8	(1.0)
Grade		
I	91	(11.4)
II	502	(62.7)
III	208	(26.0)
Nodal status		
N0	492	(61.4)
N1	226	(28.2)
N2	51	(6.4)
N3	32	(4.0)
Menopausal status		
Pre-Menopausal	167	(20.8)
Peri-Menopausal	51	(6.4)
Post-Menopausal	583	(72.8)
Receptor status		
ER+	681	(85.0)
ER-	120	(15.0)
PgR+	563	(70.3)
PgR-	238	(29.7)
HER2+	110	(13.7)
HER2-	691	(86.3)
HR+	688	(85.9)
HR-	113	(14.1)
Receptor defined subtype		
Luminal A-like	510	(63.7)
Luminal B-like (HER2 positive)	74	(9.2)
Luminal B-like (HER2 negative)	104	(13.0)
HER2 positive (non-luminal-like)	36	(4.5)
TNBC	77	(9.6)

4.1.2 Unsupervised clustering of protein expression profiles in patients with breast cancer

Michaela Bayerlová and I decided to investigate the patient profiles of 37 metabolism-related proteins by assessing their distribution via unsupervised hierarchical clustering. As a result, illustrated by the upper dendrogram coloring in Figure 10, clustering divided the whole cohort into two patient clusters (green, n = 440; violet, n = 361).

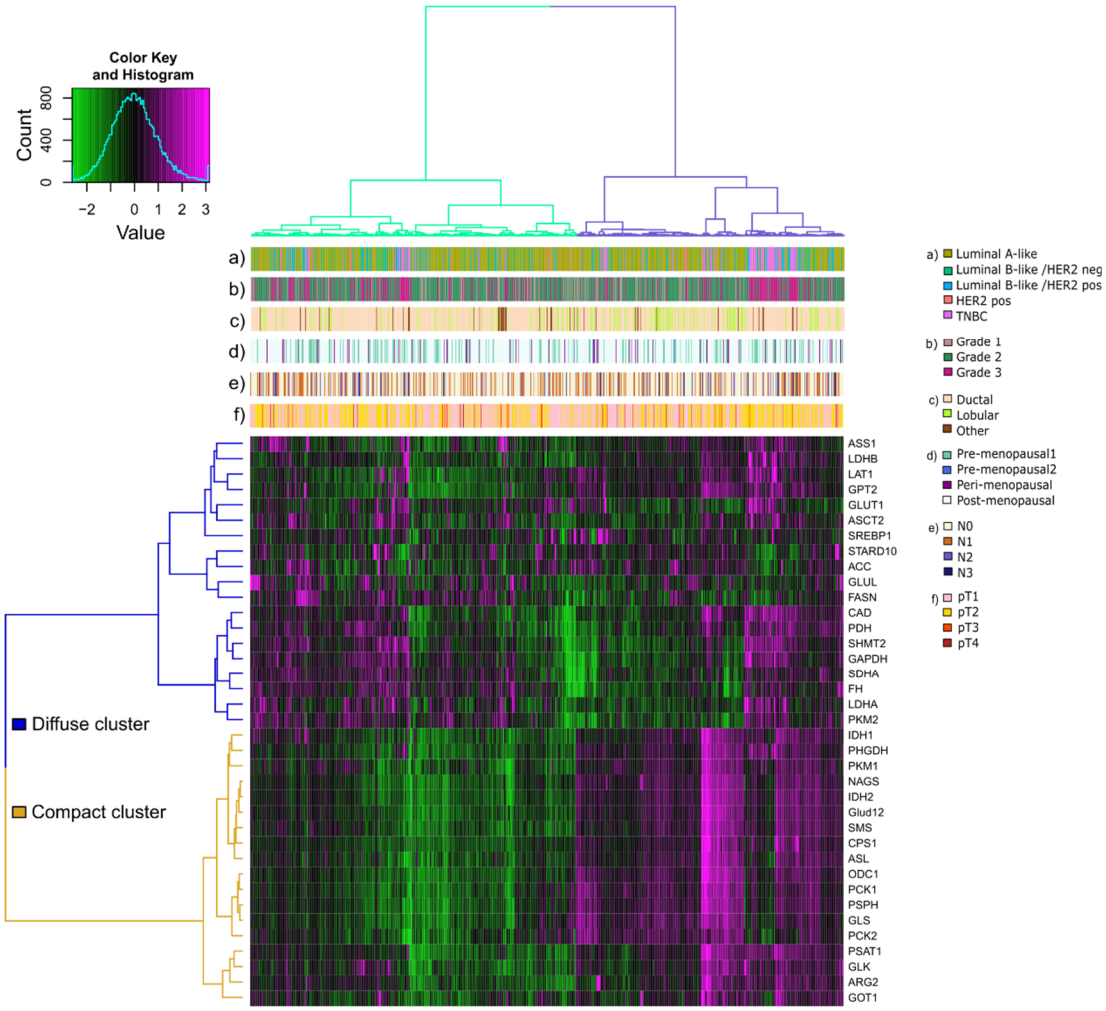

Figure 10 - Unsupervised clustering of protein profiles.

The heatmap represents expression levels of 37 metabolism related proteins after unsupervised hierarchical clustering. The data set consists of 801 tumor specimens. Z-scores of log2 transformed protein expression levels are color coded on a low-to-high scale (green – black- magenta). Dendrogram branches divide the patient set into a green and violet cluster and protein targets into a 'diffuse' and 'compact' cluster. Annotation bars include receptor defined subtypes (a); Histological grade (b); Histology (c); Menopausal status (d); Nodal status (e) and T stage (f).

As presented in Figure 10, the distribution of clinical factors (illustrated as labels a, b, c, d, e and f, above the heatmap) showed no significant association with the green and violet patient cluster.

To elucidate a potential association with survival, M. Bayerlová performed Kaplan-Meier analysis of the two patient clusters (Figure 11).

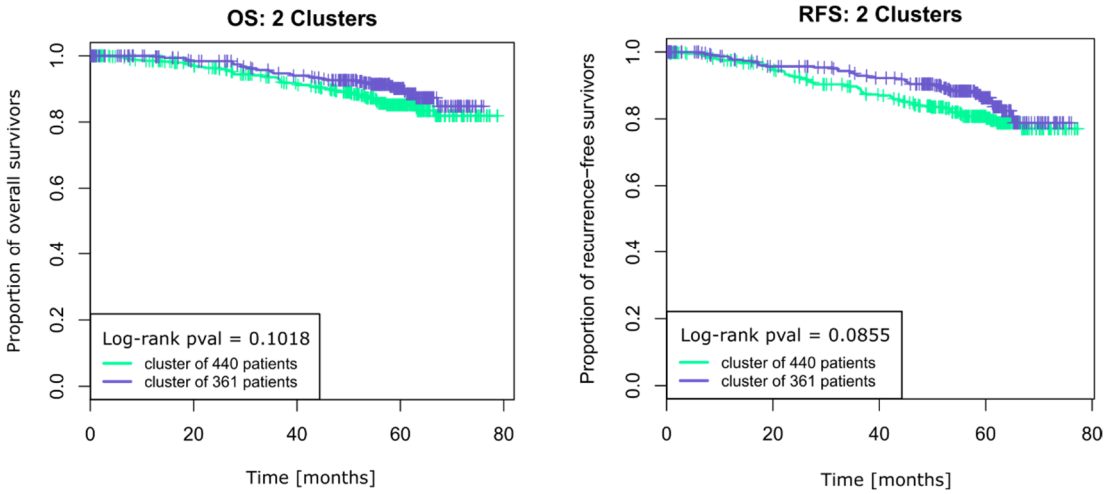

Figure 11 - Kaplan-Meier analysis of green and violet patient cluster.

Kaplan-Meier curves show proportions of overall survivors (OS) and recurrence-free survivors (RFS) of two separate clusters (green and violet). Statistical difference in outcome between Kaplan-Meier curves were compared by log-rank test. pval, p value.

As shown in Figure 11, no significant association with OS or RFS was detected. However, after observing the heatmap pattern more closely, a distinct horizontal partition of the protein targets showed up as a dominant feature of the heatmap. Furthermore, a separation into two protein expression clusters indicated a potential functional difference throughout the whole patient cohort. Therefore, I divided the protein targets by the given dendrogram (depicted on the left-hand side of the heatmap) into two protein cluster subgroups, a ‘diffuse’ cluster (blue, n = 19), characterized by a heterogeneous protein expression pattern and a ‘compact’ cluster (gold, n = 18) with clear protein expression pattern (Figure 10). Notably, the impact of the ‘compact’ protein cluster in driving the initial heatmap clustering and formation of the two patient clusters, seemed to subdue the effects of the ‘diffuse’ protein cluster. Since no differences in survival of the ‘compact’ cluster were observed, I focused on re-investigating the ‘diffuse’ protein cluster separately.

4.1.3 'Diffuse' protein signature revealed three patient clusters significantly associated with survival

Unsupervised hierarchical clustering of the 19 protein targets represented in the 'diffuse' cluster was performed over all patient specimens. Eliminating all proteins of the 'compact' cluster, resulted in a heterogenous heatmap with three refined patient clusters based on the dendrogram arrangement, depicted in blue (n = 242), yellow (n = 89) and brown (n = 470), (Figure 12A).

Based on the resulted dendrogram, the patient clusters were compared for survival analysis in terms of OS and RFS outcome. This revealed a significant difference among the clusters in both, OS ($p = 0.023$, Figure 12B) and RFS ($p = 0.0071$, Figure 12C), as illustrated in the Kaplan-Meier curves. The blue cluster showed the most favorable overall and recurrence-free survival, whereas the yellow cluster represented the least favorable outcome. Clinical parameters (age, tumor size, histology, T stage, grade, node status, menopausal status and receptor defined status) were further examined by M. Bayerlová for differences in distribution between the patient clusters. Univariate comparison across the patient's groups showed that all clinical parameters were significantly different between the three clusters ($p \leq 0.05$). Furthermore, multivariate analysis was conducted based on selected clinicopathological covariates (Appendix, Table S1).

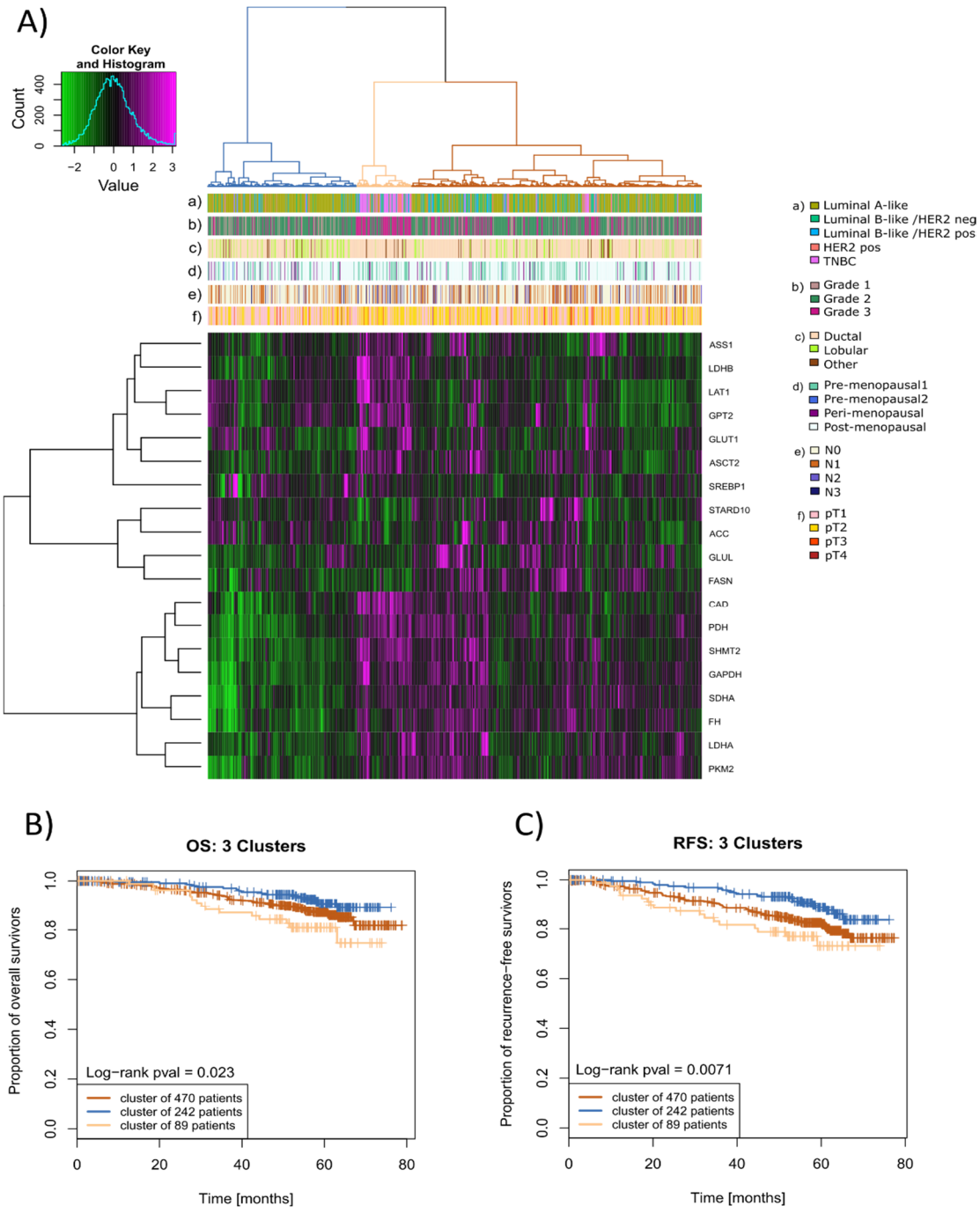

Figure 12 - Unsupervised clustering and analyses based on 'diffuse' cluster refinement.

The heatmap represents metabolism related protein expression levels of the 'diffuse' target signature after unsupervised hierarchical clustering of 801 tumor specimen. Z-scores of log2 transformed protein expression levels are color coded on a low-to-high scale (green –black-magenta). Annotation bars include receptor defined subtypes (a); Histological grade (b); Histology (c); Menopausal status (d); Nodal status (e) and T stage (f). Statistical analysis of the three patient clusters (blue, yellow, brown) is shown in the Appendix (Table S1). Kaplan-Meier curves visualize the proportion of overall survivors (B) and recurrence-free survivors (C), compared by log-rank test. pval, p value.

4.1.4 The proteomic network of the ‘diffuse’ and ‘compact’ cluster

In respect to outcome, the different clinicopathological features represented between the unique cluster separation of Figure 10 merited a deeper investigation. Therefore, I was interested in the differences between the compact and diffuse protein cluster which had resulted from the initial clustering and explored their proteomic network. To visualize the biological context of the proteins representing the ‘diffuse’ and ‘compact’ clusters at a glance, I visualized them in two protein networks by using the STRING Database (Figure 13).

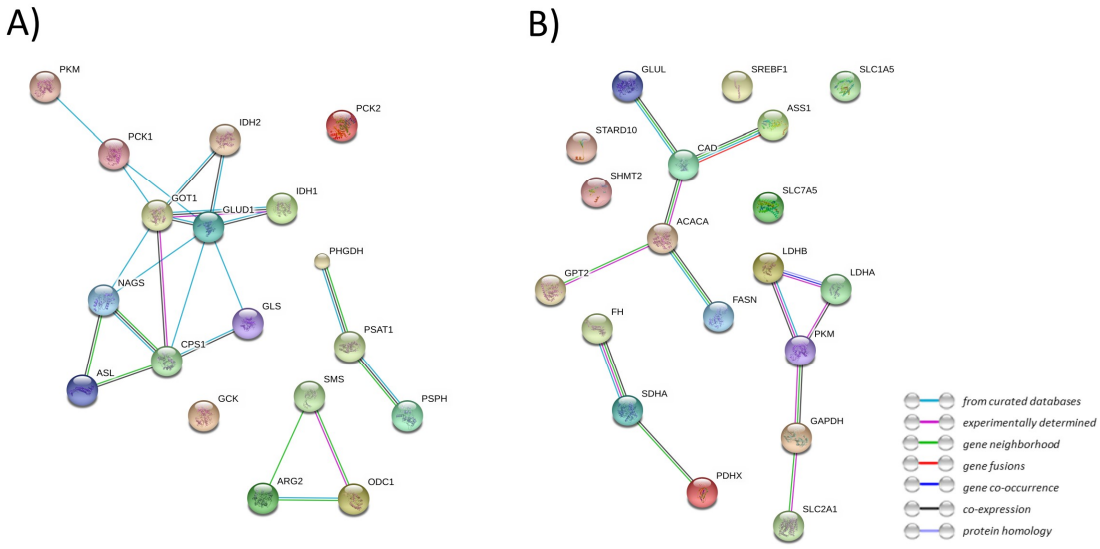

Figure 13 - Protein network visualization.

STRING illustrations are based on proteins represented in the ‘compact’ cluster subgroup (A) and proteins represented in the ‘diffuse’ cluster subgroup (B). STRING visualization was performed for each group individually and the evidence based network edges were set to an interaction score of 0.4. The given legend shows the type of interactions that were selected for the visualization.

The STRING visualization resulted in distinct interaction nodes, illustrating possible protein relations. As part of the ‘diffuse’ cluster, all proteins related to glycine synthesis (SHMT2), lipid and fatty acid synthesis (FASN, STARD10, ACACA, SREBF1), as well as glycolysis and lactate production (GLUT1, GAPDH, PKM2, LDHA, LDHB) were observed. The ‘compact’ cluster in comparison is composed of all measured proteins associated with serine synthesis (PHGDH, PSAT1, PSPH). Pyruvate kinase isozyme M1 (PKM1) was the only glycolysis related protein

represented in the ‘compact’ cluster. Proteins related to the TCA cycle, urea cycle and glutaminolysis, were found in both, the ‘diffuse’ and the ‘compact’ cluster.
In addition, I considered pathway enrichment analysis, however due to the relatively low numbers of measured proteins, M. Bayerlová could not detect any enriched pathways. Therefore, I decided to shift the main focus of the study towards biomarker discovery and further investigate the individual protein target expressions that shaped the whole initial clustering.

4.1.5 Correlations between individual target expression and clinicopathological characteristics

In order to identify individual proteins associated with survival and to evaluate their potential role as biomarkers, I next analyzed the expression of all probed proteins individually. The association of each protein expression level with OS and RFS was tested via univariate Cox proportional hazard regression models by M. Bayerlová and protein expression was treated as a continuous variable (Full table: Appendix, Table S2). Out of 37 metabolism related proteins tested, SHMT2 and ASCT2 were found to be significantly associated with overall survival (Table 3).

Table 3 - Protein targets significantly associated with overall survival (OS)

Target	HR	95 % CI	P	FDR	Affiliation
SHMT2	1.93	1.48 – 2.51	<0.001	<0.001	Serine Metabolism
ASCT2	1.83	1.39 – 2.42	<0.001	<0.001	Glutamine Metabolism

OS events: 83; p, p value; HR, Hazard Ratio; FDR, false discovery rate; CI, confidence intervals

Furthermore, univariate Cox analysis of recurrence-free survival, revealed 6 out of 37 proteins to be significantly associated with outcome (Table 4).

Table 4 - Protein targets significantly associated with recurrence-free survival (RFS)

Target	HR	95 % CI	P	FDR	Affiliation
SHMT2	1.88	1.50 – 2.36	<0.001	<0.001	Serine Metabolism
ASCT2	1.83	1.45 – 2.31	<0.001	<0.001	Glutamine Metabolism
GAPDH	1.52	1.19 – 1.94	<0.001	0.009	Glucose Metabolism
FH	1.65	1.20 – 2.27	0.002	0.019	TCA Cycle
CAD	2.07	1.29 – 3.33	0.003	0.019	Pyrimidine Metabolism
PKM2	1.46	1.13 – 1.88	0.003	0.020	Glucose Metabolism

RFS events: 109; p, p value; HR, Hazard Ratio, false discovery rate; CI, confidence intervals

After having revealed which protein expression profiles were univariately associated with survival, the breast cancer patients were grouped depending on “low” and “high” protein expression concerning these targets, to explore relationships with other clinicopathological variables. This was based on the median protein expression of SHMT2, ASCT2, GAPDH, FH, CAD and PKM2 (Appendix, Table S3). Univariate analysis showed that all six protein expression profiles were significantly associated with tumor size, T stage, grade, nodal status and receptor defined subgroups. Except for CAD, all proteins showed a significant association with histology, whereas PKM2 displayed the only protein profile that significantly correlated with age. No significant difference between protein expression and menopausal status was observed.

4.1.6 SHMT2 and ASCT2 protein expression as independent prognostic factors in patients with breast cancer

To confirm the findings, multivariate Cox analyses for overall and recurrence-free survival was performed based on selected clinicopathological covariates and univariate significance. Proteins showing significance in the univariate Cox analysis were included (Full table: Appendix, Table S4).

Table 5 - Univariate and Multivariate Cox regression analysis of overall survival

Characteristics	Univariate analysis	SHMT2		ASCT2	
		Multivariate analysis		Multivariate analysis	
	p	Hazard Ratio (95% CI)	p	Hazard Ratio (95% CI)	p
Protein expression high vs. low		1.53(1.10-2.12)	0.011	1.23(0.90-1.68)	0.194
Age at surgery (years)	<0.001	1.06(1.03-1.09)	<0.001	1.06(1.03-1.08)	<0.001
Tumor size	<0.001	*Not included*		*Not included*	
< 2cm					
≥ 2-5cm					
> 5cm					
Histology	0.306	*Not included*		*Not included*	
Ductal vs. non-ductal					
T stage	<0.001				
T1 vs. ≥T2		1.46(0.88-2.40)	0.141	1.49(0.90-2.47)	0.123
Grade	<0.001				
I		*Reference*		*Reference*	
II		1.69(0.52-5.49)	0.385	1.77(0.54-5.76)	0.345
III		2.40(0.70-8.23)	0.163	2.95(0.87-9.99)	0.081
Nodal status	<0.001				
N0 vs. ≥N1		1.86(1.18-2.92)	0.007	1.85(1.17-2.92)	0.008
Menopausal status	0.001				
Pre-/Peri- vs. Post-Menopausal		0.72(0.28-1.85)	0.489	0.80(0.31-2.05)	0.640
Receptor status					
ER- vs. ER+	<0.001	*Not included*		*Not included*	
PgR- vs. PgR+	<0.001	*Not included*		*Not included*	
HER2- vs. HER2+	0.682	*Not included*		*Not included*	
HR- vs. HR+	<0.001	0.72(0.42-1.22)	0.217	0.63(0.37-1.06)	0.082
Receptor defined subtypes	<0.001	*Not included*		*Not included*	
Luminal A-like					
Luminal B-like (HER2 positive)					
Luminal B-like (HER2 negative)					
HER2 positive (non-luminal-like)					
TNBC					

CI, confidence interval; A p value < 0.05 is considered statistically significant

Table 6 - Univariate and Multivariate Cox regression analysis of recurrence-free survival

Characteristics	Univariate analysis	SHMT2		ASCT2	
		Multivariate analysis		Multivariate analysis	
	p	Hazard Ratio (95% CI)	p	Hazard Ratio (95% CI)	p
Protein expression high vs. low		1.54(1.16-2.04)	0.003	1.31(1.01-1.71)	0.042
Age at surgery (years)	<0.001	1.04(1.02-1.07)	<0.001	1.04(1.02-1.06)	<0.001
Tumor size	<0.001	*Not included*		*Not included*	
< 2cm					
≥ 2-5cm					
> 5cm					
Histology	0.110	*Not included*		*Not included*	
Ductal vs. non-ductal					
T stage	<0.001				
T1 vs. ≥T2		1.77(1.15-2.74)	0.010	1.80(1.16-2.80)	0.009
Grade	<0.001				
I		*Reference*		*Reference*	
II		1.79(0.65-4.98)	0.262	1.85(0.66-5.14)	0.240
III		2.18(0.75-6.35)	0.154	2.64(0.92-7.59)	0.072
Nodal status	<0.001				
N0 vs. ≥N1		1.62(1.10-2.40)	0.015	1.59(1.07-2.35)	0.021
Menopausal status	0.010				
Pre-/Peri- vs. Post-Menopausal		0.65(0.31-1.38)	0.263	0.73(0.35-1.54)	0.410
Receptor status					
ER- vs. ER+	<0.001	*Not included*		*Not included*	
PgR- vs. PgR+	<0.001	*Not included*		*Not included*	
HER2- vs. HER2+	0.489	*Not included*		*Not included*	
HR- vs. HR+	<0.001	0.79(0.49-1.27)	0.334	0.69(0.43-1.10)	0.115
Receptor defined subtypes	<0.001	*Not included*		*Not included*	
Luminal A-like					
Luminal B-like (HER2 positive)					
Luminal B-like (HER2 negative)					
HER2 positive (non-luminal-like)					
TNBC					

CI, confidence interval; A *p value* < 0.05 is considered statistically significant

The analyses of the association between SHMT2/ASCT2 protein expression levels and clinical characteristics of BC via multivariate Cox models was conducted to address the question whether SHMT2 and ASCT2 protein expression are independent prognosticators for OS and RFS. This revealed, that high SHMT2 protein expression is indeed an independent negative prognostic factor for OS (p = 0.011; Table 5) and

both, high SHMT2 and high ASCT2 protein expression levels are independent negative prognostic factors for RFS (SHMT2, p = 0.003; ASCT2, p = 0.042; Table 6) in BC patients. Kaplan–Meier survival estimates, based on dichotomized protein expression data, subsequently confirmed that BC patients with high SHMT2, as well as high ASCT2 protein expression presented a significantly unfavorable OS time (SHMT2, p = <0.001; ASCT2, p = 0.0165) and RFS time (SHMT2, p = <0.001; ASCT2, p = <0.001), (Figure 14).

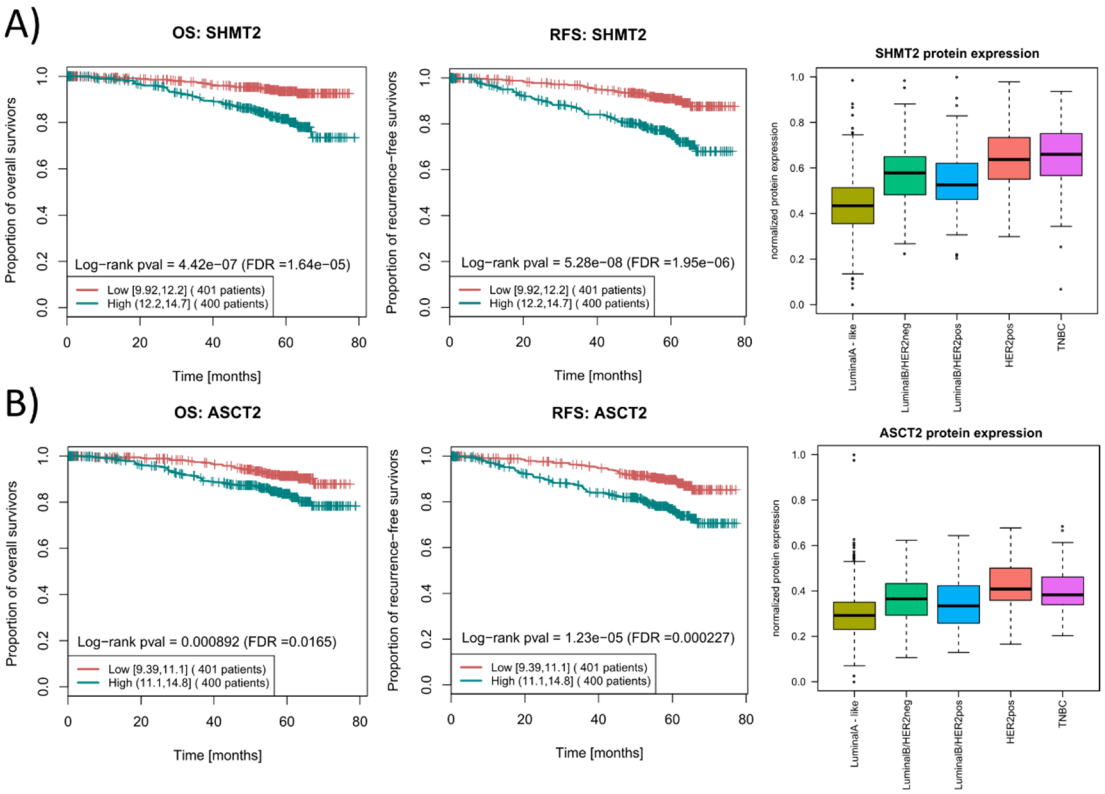

Figure 14 - Kaplan-Meier survival estimates and boxplot representation of key targets associated with survival.

Kaplan-Meier plots of SHMT2 and ASCT2 for overall survival (OS), (A), and recurrence-free survival (RFS), (B). Statistical difference in outcome between high (n = 400) and low (n = 401) protein expression were compared by log-rank test. Boxplots represent the relative target protein expression per receptor defined subtype, Luminal A-like (n = 510), Luminal B-like HER2neg (n = 104), Luminal B-like HER2pos (n = 74), HER2pos (n = 36), TNBC (n = 77). FDR, false discovery rate; pval, p value.

Additionally, I explored the distribution of SHMT2 and ASCT2 protein expression across BC subtypes. This revealed a higher protein expression of both targets in the

aggressive HER2 positive and the triple negative (TNBC) breast cancer subtype, as compared to the luminal subgroups (Figure 14).

In collaboration with PD Dr. med. Jörg Buchmann of the Institute of Pathology, Hospital Martha-Maria (Halle(Saale), DE), the results from my screen were confirmed in clinical practice via SHMT2 and ASCT2 immunostaining of representative cases. As illustrated in Figure 15, the cases selected on the basis of the RPPA data are in line with the observed cellular target expression pattern of SHMT2 and ASCT2. Cases of high target protein expression in RPPA also represented a high cellular target protein expression in IHC and vice versa.

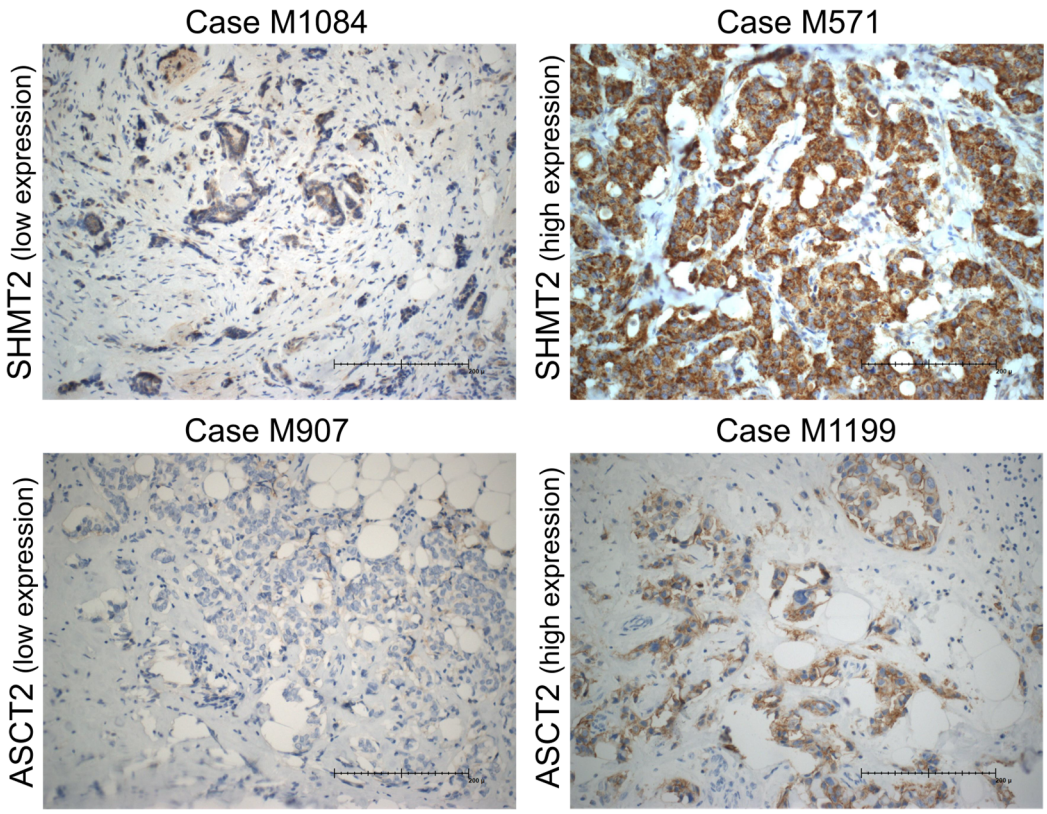

Figure 15 - Representative immunoexpression of SHMT2 and ASCT2.

Cases were selected on basis of RPPA protein expression results. The figure shows representative pictures of the highest or lowest 10% cases based on the target expression over all cases. SHMT2 immunoexpression is elevated in Case M571 and low in Case M1084. ASCT2 immunoexpression is elevated in Case M1199 and low in Case M907. The scale bar indicates 200 µm (20x).

Taken together, these results illustrate the prognostic value of profiling proteome data and highlight the importance of the proteomic level in biomarker research. All presented results are further discussed in Chapter 5.

4.2 Proteomic profiling of metabolic adaptations in hypoxic conditions

4.2.1 Experimental rationale and generation of linear regression model

In order to approach the proteomic profiling of metabolic changes under dynamic hypoxic conditions, I used 4 different breast cancer cell lines (MCF-7, SKBR3, MDA-MB-231 and MDA-MB-468) for my perturbation experiments. All cell lines were treated individually under the same conditions. The cell lines were incubated in normoxic (21% O_2), mild hypoxic (1.2% O_2), strong hypoxic (0.2% O_2) and MIMIC conditions (200µM $CoCl_2$) in a time dependent manner. The protein was harvested after 0h, 6h, 18h and 24h of incubation and after a 2h re-oxygenation at 26h. To obtain quantitative expression data, the protein lysates were further processed via RPPA and protein array slides were probed with antibodies targeting 40 metabolism related proteins. Thereby, the selected set of protein targets reflects the full spectrum of metabolism related proteomic targets used in the breast cancer patient's cohort and three additional proteins of interest. The full list of antibodies used during my projects is illustrated in Chapter 3, Section 3.1.5. After performing the raw data analysis and quality control, I reached out to investigate the data in more depth and collaborated with Christian Tönsing of the Institute of Physics at the University of Freiburg (DE). Together, we decided to create a linear regression model (LRM) of the data matrix in order to statistically define which target expression is altered under the given conditions.

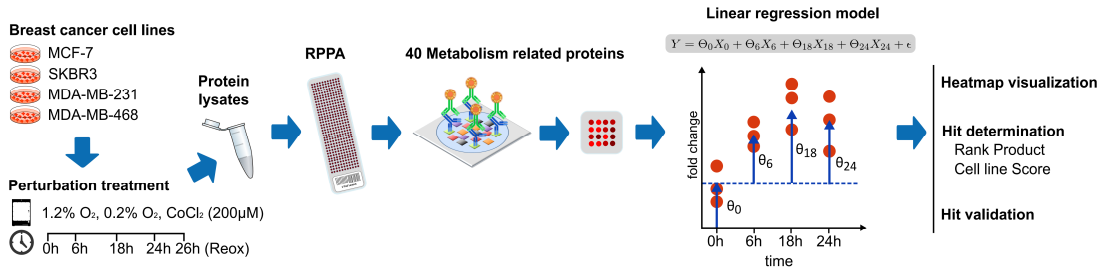

Figure 16 - Experimental workflow.

Schematic presentation of the experimental workflow and analysis.

The preprocessed RPPA time course data with biological triplicates for each time point were analyzed by C. Tönsing individually for each of the target proteins and for each of the 12 combinations of cell lines and treatments. A linear regression model was used for the log2 signal intensities of the target protein time courses and cell line-treatment combination individually, to merge the replicates and asses the kind and strength of regulation. ANOVA was applied to each time course in order to discriminate between a constant time course signal at the basal expression level of the target protein and significantly regulated expression profiles ($p < 0.05$). The linear regression model further served to illustrate the data and for approaches to determine top-regulated targets. The experimental workflow is depicted in Figure 16.

4.2.2 Heatmap representation of the dataset via a linear regression model

In a first step, the linear regression model was used to visualize the whole data set. Therefore, target protein regulation profiles were assigned based on time point specific regulation strengths from the LRM. Only significantly regulated estimates with $p[t\{6,18,24\}] < 0.05$ compared to the basal expression level were used to identify either a up or down regulation. Time courses with one, two or three significantly up-regulated time points were assigned to expression profiles ‘one up’, ‘two up’ and ‘all up’, respectively and likewise for down-regulated signals. Time courses with alternating sign, i.e. a significant down-regulation followed by a not significant regulation and further by a significant up-regulation were specified as ‘down-up’, while the opposite was termed as ‘up-down’. A double sign-change of significantly regulations, e.g. ‘up-down-up’ was not observed in the dataset. All other time courses with no significant regulation were assigned to ‘constant’ profiles. The resulting heatmap represents all target protein regulation profiles per cell line and condition (Figure 17). The corresponding color coding is displayed and explained in the corresponding legend.

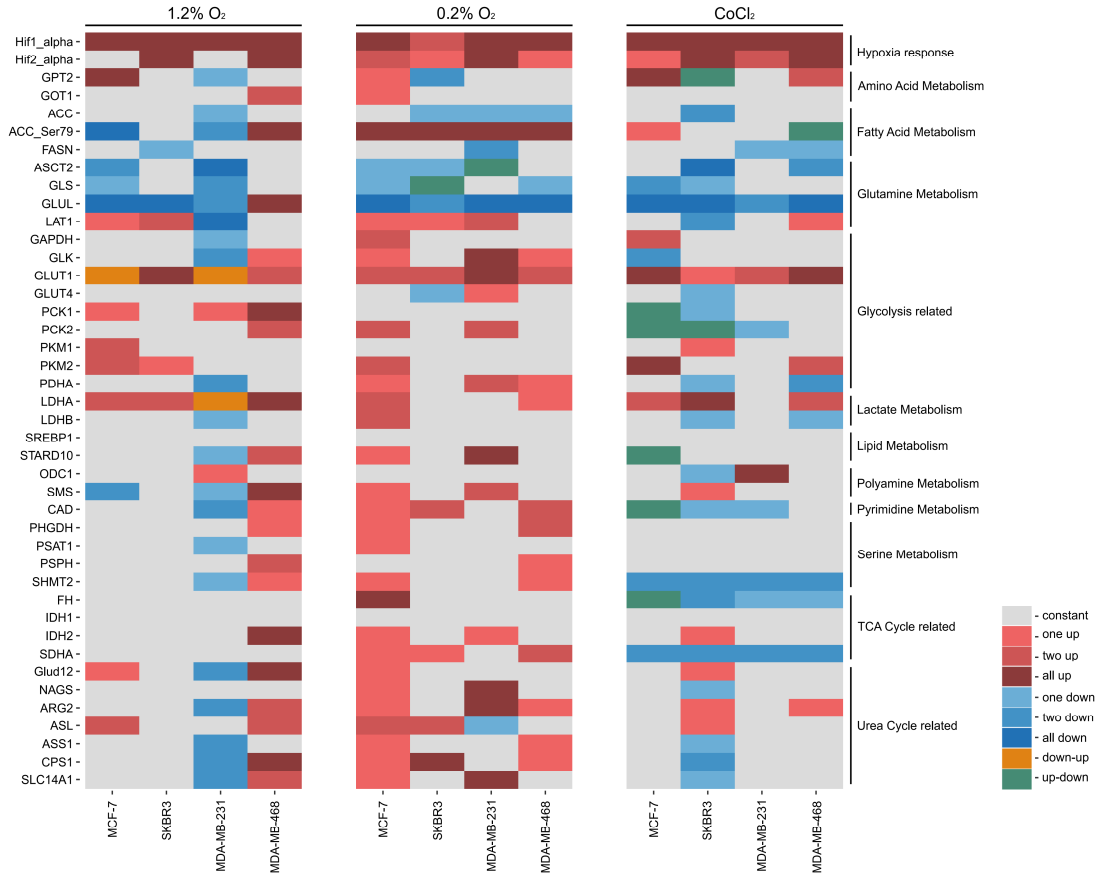

Figure 17 - Heatmap visualization of protein time course profiles.

The heatmap represents the condensed time course data of each target on the basis of the linear regression model results. Protein target expression direction, during treatment exposure is color coded and clarified in the figure legend on the right-hand side.

As a result, the heatmap showed a quite diverse pattern. Nevertheless, the behavior of HIF-1α, displayed as upregulated in all hypoxic and mimic conditions and over all cell lines, confirmed the power of the LRM and its visualization. No obvious pattern of a whole metabolic pathway matching with a treatment condition could be observed. However, individual target regulation profiles (e.g. GLUT1) seemed to be heavily influenced in all hypoxic conditions and cell lines. Therefore, I decided to statistically approach the data set in order to elucidate individual top-regulated targets.

4.2.3 Identification of top-regulated target proteins

Given the complex picture of the heatmap visualization, two different statistical approaches were utilized to investigate the top-regulated target proteins. First, I

analyzed top-regulated targets via a 'Cell line (Cl) score' (Figure 18A). The Cl Score enables the identification of top-regulated target proteins in all cell lines and treatment combinations. For each treatment, the Cl Score indicates the number of target proteins, with expression time courses indicating for a significant regulation throughout all cell lines. A pANOVA of < 0.05 has to be fulfilled by a target protein expression time course of a cell line/treatment combination to be identified as significantly regulated. A Cl Score of 0 indicates the number of target time courses which are not significantly regulated in any cell line, whereas a Cl Score of 1 indicates the number of target time courses significantly regulated in 1 cell line, a Cl Score of 2 in 2 cell lines, a Cl Score of 3 in 3 cell lines and a Cl Score of 4 in all four cell lines. The full data matrix of Figure 18A can be found in the Appendix (Table S6).

Next, C. Tönsing used a different second indicator for top-regulated target proteins, a regulation ranking combined by the rank product [139]. For this, target proteins were ranked by two measures to obtain the strength of the regulation for each combination of cell line and treatment individually. The first measure is the summed square of residuals (SSR) from the ANOVA, if pANOVA < 0.05 which is sensitive for sustained expression profiles. The second measure ranks the target proteins by the absolute value of the maximal time point specific regulation in the time course and thus takes account of peaked expression profiles. The two rankings are combined by the rank product for each cell line and treatment combination. The 'rank by treatment' contains rank product combinations in all cell lines, for each treatment individually. In a last step, treatment ranks were combined by the rank product yielding the 'overall rank'. A low rank number thereby indicates a high ranked target, whereas a high rank number indicates a low ranked target (Figure 18B).

A

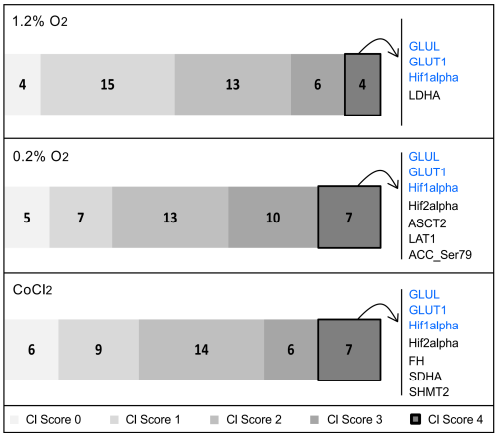

B

Target	Overall rank	Rank per treatment 1.2% O_2	0.2% O_2	$CoCl_2$	Affiliation
Hif1_alpha	1	1	1	1	Hypoxia Response
GLUT1	2	3	3	5	Glycolysis related
LDHA	3	2	8	4	Lactate Metabolism
GLUL	4	5	9	2	Glutamine Metabolism
Hif2_alpha	5	10	5	3	Hypoxia Response
LAT1	6	4	4	12	Glutamine Metabolism
ACC_Ser79	7	8	2	23	Fatty Acid Metabolism
PCK1	8	6	20	6	Glycolysis related
ASCT2	9	9	17	8	Glutamine Metabolism
CAD	10	19	10	7	Pyrimidine Metabolism
GLK	11	11	6	28	Glycolysis related
PDHA	12	16	12	18	Glycolysis related
IDH2	13	22	11	17	TCA Cycle related
GLS	14	26	7	21	Glutamine Metabolism
GPT2	15	21	16	10	Amino Acid Metabolism
SMS	16	7	23	24	Polyamine Metabolism
SDHA	17	n.s.	22	9	TCA Cycle related
PKM2	18	13	18	14	Glycolysis related
CPS1	19	28	14	15	Urea Cycle related
GAPDH	20	12	19	22	Glycolysis related
SHMT2	21	17	37	11	Serine Metabolism
ARG2	22	29	13	27	Urea Cycle related
PCK2	23	27	27	13	Glycolysis related
GOT1	24	14	25	n.s.	Amino Acid Metabolism
PSAT1	25	15	24	n.s.	Serine Metabolism
PKM1	26	18	n.s.	20	Glycolysis related
FH	27	n.s.	33	16	TCA Cycle related
FASN	28	n.s.	15	32	Fatty Acid Metabolism
Glud12	29	20	28	30	Urea Cycle related
NAGS	30	33	21	25	Urea Cycle related
ODC1	31	31	n.s.	19	Polyamine Metabolism
ASL	32	24	36	29	Urea Cycle related
STARD10	33	25	29	34	Lipid Metabolism
LDHB	34	23	31	35	Lactate Metabolism
ASS1	35	35	26	26	Urea Cycle related
GLUT4	36	n.s.	30	33	Glycolysis related
SLC14A1	37	32	34	36	Urea Cycle related
ACC	38	34	35	31	Fatty Acid Metabolism
PSPH	39	30	n.s.	n.s.	Serine Metabolism
PHGDH	40	n.s.	32	n.s.	Serine Metabolism
SREBP1	n.s.	n.s.	n.s.	n.s.	Lipid Metabolism
IDH1	n.s.	n.s.	n.s.	n.s.	TCA Cycle related

C

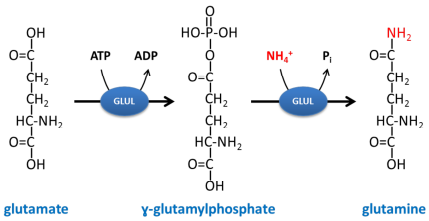

Figure 18 - Determination of top-regulated protein targets.

Illustrated are the results from the Cell line (Cl) Score analysis (A) and the rank product analysis (B). Furthermore, the reaction of one of the top-targets GLUL is shown in (C).

As presented in Figure 18A, the highest Cl Score was presented by 4 target time courses in the mild hypoxic condition (1.2% O_2), 7 target time courses in the strong hypoxic condition (0.2% O_2) and 7 targets in the MIMIC condition (200µM $CoCl_2$). As highlighted in blue, it was striking that out of all targets, three target time courses (HIF1_alpha, GLUT1 and GLUL) were found to be significantly regulated in all treatment conditions and all four cell lines. This observation was further validated by the second approach, the rank product, were HIF1_alpha, GLUT1 and GLUL achieved the highest 'Overall ranks' together with LDHA.

In order to provide an in-depth view on the top-targets during hypoxia exposure, the time course data of each target were extracted and depicted in Figure 19.

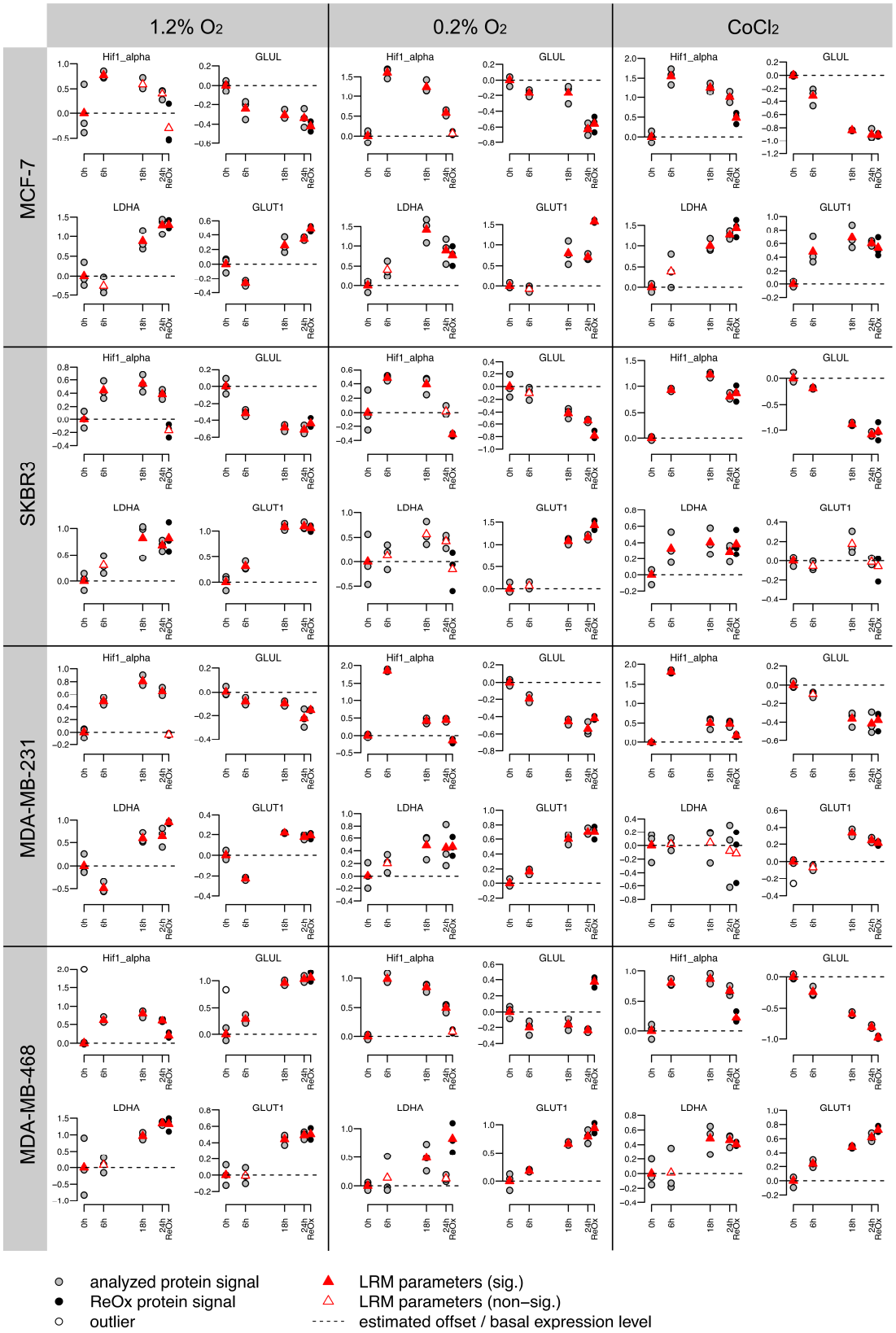

Figure 19 - LRM and time course data of top-regulated protein targets.

Illustrated are the time course data of HIF1_alpha, GLUL, LDHA and GLUT1 per condition and cell line. Indicators for protein signals and LRM parameters are described in the legend.

As shown in Figure 19, the protein expression of the hypoxia-inducible factor 1 alpha is elevated under hypoxic conditions in all cell lines and conditions. This observation confirms the experimental design and analysis. Further, the protein expression profiles of GLUT1 and LDHA were found to be mostly elevated under hypoxic conditions, whereas GLUL protein expression levels were mostly down regulated. Since HIF-1α served as internal control and GLUT1 and LDHA are known to be effected by hypoxic conditions, which I will further discuss in Chapter 5, I decided to follow up on the novel connection of hypoxia and GLUL in breast cancer. The glutamate-ammonia ligase (GLUL) pathway is illustrated in Figure 18C.

4.2.4 GLUL expression profile

After elucidating GLUL as one of the top-regulated targets during hypoxia exposure, I next wanted to know how the expression profile of GLUL is represented in breast cancer patients. Therefore, I used The Cancer Genome Atlas (TCGA) data which was conducted on primary breast cancer tumor specimen with both RNA-sequencing data and clinical annotations. Normalized gene expression data from the cBioPortal website was obtained, log2 transformed and filtered for the genes of interest. Further, a one-way analysis of variance (ANOVA), was conducted to differentiate between breast cancer subtypes. The gene expression profile of GLUL in different breast cancer subtypes is shown in Figure 20.

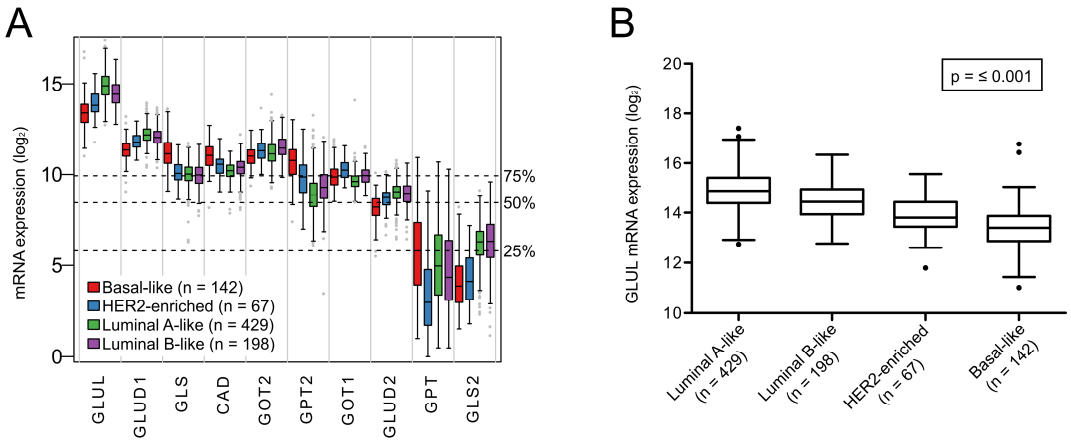

Figure 20 - GLUL expression profile.

Boxplots represent the log2 GLUL gene expression in comparison to other glutamine related targets (A) and across different breast cancer subtypes (B). p, p value.

Interestingly, GLUL mRNA expression was found to be the highest among all glutaminolysis related genes in the TCGA dataset (Figure 20A). Furthermore, GLUL gene expression was significantly different between the BC subtypes and higher in the luminal breast cancer subtype in comparison to the basal subtype (Figure 20B).
As reported in Chapter 1, hypoxic conditions and the basal breast cancer subtype are associated with a poorer prognosis in comparison to well oxygenized tumors and the luminal subtype.

4.2.5 GLUL survival association

After observing decreased protein expression of GLUL under hypoxic conditions and lower gene expression in the basal subtype, I was interested to investigate the impact of GLUL expression on overall survival (OS) and recurrence-free survival (RFS).
I performed Kaplan-Meier survival analysis in terms of OS and RFS outcome. This revealed a significant difference between high and low GLUL gene expression in both, OS ($p = 0.0027$, Figure 21A) and RFS ($p = 0.0173$, Figure 21B), as illustrated in the Kaplan-Meier curves. High GLUL expression showed the most favorable OS and RFS, whereas low GLUL expression represented the worst.
Furthermore, the correlation of GLUL gene expression with the Tumor (T) stage was analyzed. As shown in Figure 21C, lower GLUL expression is significantly correlated with a higher T stage and vice versa. Moreover, GLUL mRNA expression in high and low HIF-1α expressing subgroups of breast cancer cases were analyzed. As shown in Figure 21D, GLUL expression is significantly elevated in the HIF-1α low patient subgroup whereas low GLUL expression is associated with the HIF-1α high expressing patient subgroup.
In conclusion, after I generated dynamic time course data of 40 metabolic proteins under hypoxic and MIMIC conditions, C. Tönsing and I were able to provide an overview of significant changes in protein regulation profiles under the given conditions and further elucidated top-regulated targets. With a focus on the novel associations of the hypoxic driven GLUL expression changes, I elaborated on clinical correlations with GLUL. All results are further discussed in Chapter 5.

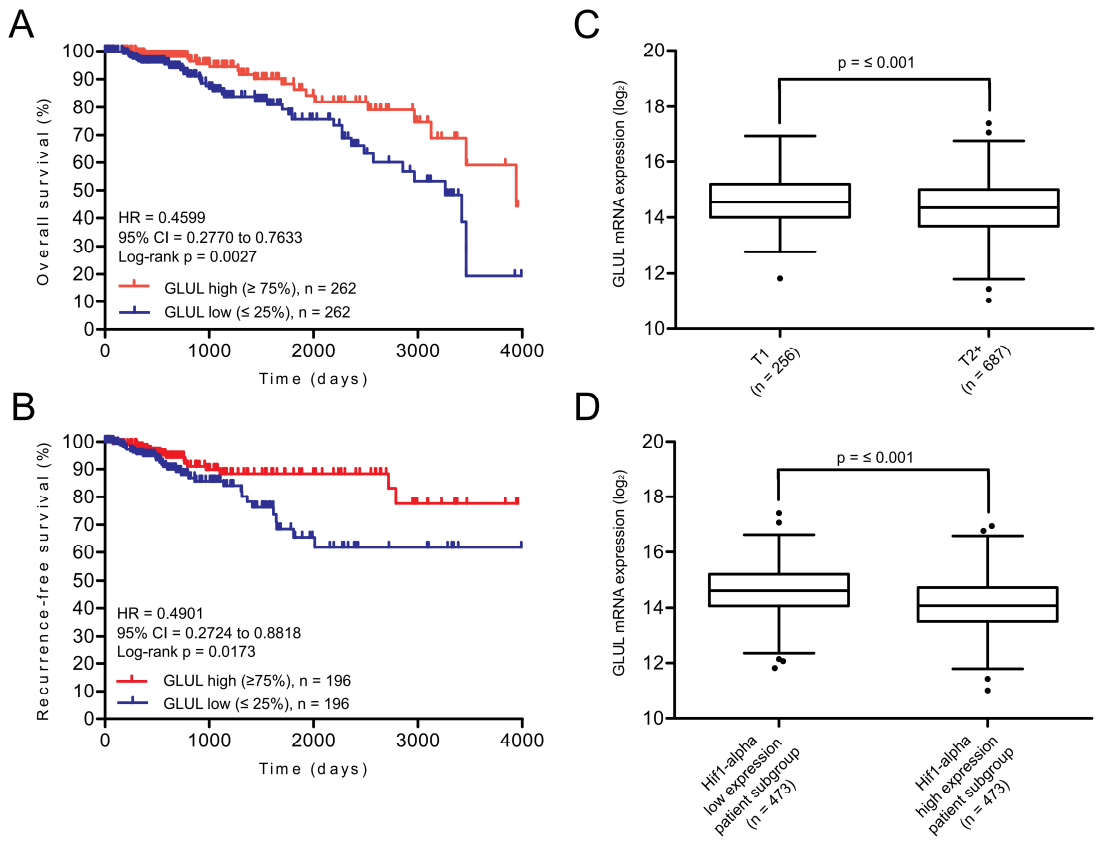

Figure 21 - Kaplan-Meier survival estimates of GLUL gene expression and boxplot representation of T stage and HIF1-alpha association.

Kaplan-Meier plots of GLUL for overall survival (OS), (A), and recurrence-free survival (RFS), (B). Statistical difference in outcome between high and low gene expression were compared by log-rank test. Boxplots represent the target gene expression in association to T stage (C) and HIF1-alpha expression subgroups (D). p, p value.

Chapter 5

Discussion

Since breast tumors are heterogenous at the molecular level and in patient outcome, clinical management includes an individual tumor characterization, which leads to personalized treatment decisions. However, this is mostly based on the measurement of few parameters, i.e. gene/protein expression status of ER, PR, and HER2. So far, the metabolic state of tumors has not been widely studied and is insufficiently covered with current molecular biomarkers that are predictive for clinical outcome. Even though RNA does inform on phenotypic characteristics, genomic and transcriptomic screens of BC patient tumors have thus far proven unsuccessful to predict protein states [140], [141]. Therefore, complementary studies investigating the metabolic landscape of breast cancer at the proteomic level should be superior in identifying metabolism based biomarkers with clinical impact.

5.1 Proteomic profiling of breast cancer metabolism identifies SHMT2 and ASCT2 as prognostic factors

In the first part of my PhD project, I wanted to assess the relationship between protein profiles of major metabolic targets/pathways and their potential prognostic value in breast cancer patients.

As a first result, cluster analysis of the generated dataset separated the metabolism associated proteins into a ‘diffuse’ and a ‘compact’ protein cluster, indicating different metabolic profiles. STRING visualization results of the protein distribution depicted a prominent role of glycolysis and lactate production in the ‘diffuse’ cluster. Also, SHMT2, primarily responsible for glycine synthesis from serine, was part of the ‘diffuse’ cluster, whereas all proteins of the serine pathway (PHGDH, PSAT1, PSPH) were part of the ‘compact’ cluster. Interestingly, key enzymes of the TCA cycle, crucial for citrate production like FH and SDHA, were present in the ‘diffuse’ cluster, whereas IDH1 and IDH2, which mainly drive the TCA cycle towards α-ketoglutarate production were part of the ‘compact’ cluster. This observation was supported by the presence of PDH, STARD10 as well as FASN in the diffuse cluster and hints towards a distinct citrate production in order to fuel the lipid and fatty acid synthesis. Mullen et al. reported in 2011 this metabolic flexibility in cancer cells. Normally, cells

condense glutamine-derived oxaloacetate with glucose-derived acetyl-CoA to produce citrate, whereas cells with defective mitochondria reverse part of their citric acid cycle using NADPH dependent isocitrate dehydrogenases (IDHs) to convert a-ketoglutarate to isocitrate via reductive carboxylation. Therefore, glutamine can reverse citric acid cycle reactions, such that reductive carboxylation yields acetyl-CoA for lipid synthesis. Despite the association between defective mitochondria and oncogenesis, the authors highlight the central importance of mitochondria in cancer, even when theses do not generate ATP [142].

Notably, the glutamine transporters ASCT2 (SLC1A5) and SLC7A5, as well as the glutamine producing enzyme GLUL, were also part of the 'diffuse' cluster. Altogether, the protein composition of the 'diffuse' cluster points towards glucose consumption, glutamine addiction and glycine production and indicates a more active Warburg like characteristic in comparison to the 'compact' cluster [51].

Following up on the 'diffuse' protein cluster, subsequent clustering analysis identified three patient clusters, which are significantly associated with survival. These three patient clusters do not fully reflect the receptor defined subtypes of BC and may thus provide a different angle towards understanding breast cancer heterogeneity. Interestingly, further analysis showed, that all proteins that were found to be significantly correlated with survival were part of the 'diffuse' cluster. SHMT2, ASCT2, GAPDH, FH, CAD and PKM2 were univariately associated with RSF and SHMT2, as well as ASCT2 with OS. Consequently, an exploration of the biomarker potential of these proteins in multivariate cox analyses was conducted.

Multivariate analysis identified SHMT2 and ASCT2 protein expression levels to be significantly associated with age, nodal status, and T Stage (RFS only). Moreover, high SHMT2 protein levels were significantly associated with poor RFS and OS. Furthermore, high protein expression of ASCT2 was significantly correlated with poor RFS. Patients of HER2 positive and HR-negative breast cancer demonstrated increased SHMT2 and ASCT2 levels compared to luminal-like patients. Notably, the significant correlation of ASCT2 and SHMT2 with nodal status, T stage as well as survival, indicates a connection between higher metabolic activity and associated protein expression in metastatic and further progressed tumors. These observations are in line with previous studies reporting that metabolic demands of cancer cells are related to their cell size, progression and protein synthesis rates [143].

Glutamine metabolism is considered to be a therapeutic target, as some cancer cells exhibit high uptake of this non-essential amino acid [51]. Recent studies have demonstrated that the primary glutamine transporter, ASCT2, promotes tumor cell survival, growth and cell cycle progression in neuroblastoma, colorectal cancer, prostate cancer, clear-cell renal cell carcinoma and non-small cell lung cancer [144], [145], [146], [147], [148]. Consequently, ASCT2 has gained more attention during the last years as its ubiquitous tissue expression, along with its ability to transport crucial amino acids, indicates a central role in physiological processes including glutamine homeostasis, embryogenesis, retroviral infection and cancer development [149], [150], [151]. Glutamine is not only an important nutrient for cancer cell survival, but also a crucial mediator for immune cell functions. ASCT2 was shown to be involved in inflammatory T cell responses, which might exert key functions in tumor immunity [152]. ASCT2 regulates the cellular uptake and concentration of nutrients and several studies indicate that blocking glutamine uptake might be an attractive strategy for cancer therapy [153], [154]. The presented results showed that high protein levels of ASCT2 are correlated with unfavourable prognosis for breast cancer patients. Along these lines, blocking the glutamine uptake by utilizing ASCT2 as a potential therapeutic target and reducing its protein expression, could be a promising approach. In addition to glutamine, the serine and glycine metabolism is also crucial in cancer cell development. Serine and glycine are biosynthetically linked and, besides cancer growth, also affect the cellular antioxidative capacity, thus supporting tumor homeostasis. SHMT2 has been implicated as an essential factor in serine and glycine metabolism in several cancer cell types, including breast cancer [62]. SHMT2 catalyzes the reversible reaction of serine and tetrahydrofolate to glycine and 5,10-methylene tetrahydrofolate. Studies have shown that high levels of glycine are associated with poor prognosis in breast cancer, irrespective of the ER status [155]. I demonstrated that high protein levels of SHMT2 are correlated with poor outcome in breast cancer patients. Inhibition of glycine synthesis by reducing SHMT2 protein expression, could therefore, represent a new treatment strategy to employ SHMT2 as a potential therapeutic target. Notably, to date there are no SHMT2 and ASCT2 inhibitors available for cancer therapy and to my best knowledge these are the first observations to report the prognostic value of SHMT2 and ASCT2 at the protein expression level in breast cancer patients.

5.2 Hypoxic regulation of metabolism associated enzymes in breast cancer

The criteria to be used in evaluating tumor metabolism are still not well established and universally applied. Furthermore, it is mostly unclear how metabolic characteristics are influenced by tumor microenvironmental factors like hypoxia and how this might influence tumor development. Therefore, it is necessary to obtain a better understanding of molecular mechanisms underlying the heterogeneity of breast cancer metabolism in different microenvironmental milieus.

In the second part of my PhD project, I thus investigated the time dependent expression changes of metabolism related proteins under different hypoxic conditions. Therefore, I generated proteomic time course data using RPPA.

In a first approach, the data was visualized using a unique heatmap method that showed an upregulation of HIF-1α in all hypoxic and mimic conditions and over all cell lines, confirming the experimental procedure and the LRM. Interestingly, the heatmap pattern revealed a very diverse picture of all protein expression time courses tested. I did not observe an obvious connection of any metabolic pathway matching a certain treatment condition. Rather, the response patterns hint towards cell line diversity as the most prominent feature, reflecting the heterogenous nature of metabolic activities. Different tumor cells seem to preferentially utilize particular catabolites. Experimental models in ovarian, prostate and breast carcinomas have also revealed a metabolic coupling of stromal and cancer cells leading to diverse metabolic profiles [156], [157]. Genomic and metabolic differences throughout all cell types might, therefore, also result in a different adaption to oxygen deprivation. These observations cloud be the reasoning for the diverse behavior across all cell lines. However, a minority of individual target regulation profiles seemed to be changed in all conditions and cell lines. Consequently, I next elucidated individual top-regulated targets. Two different approaches were used in order to confirm the results. Since, similar to the heatmap approach, no standard procedure was available to assess the data sufficiently, a Cell line (Cl) Score was generated. Scoring the target time courses identified HIF-1α, GLUT1 and GLUL as significantly regulated in all cell lines and treatment conditions.

Furthermore, besides a high rank of LDHA, also HIF-1α, GLUT1 and GLUL showed the highest overall ranks in the rank product approach. These observations not only highlight the importance of the given targets as significantly affected under hypoxic conditions, it further confirms the results and the robustness of the methods used. Further investigation explored all time courses of the top regulated targets individually and found the protein expression of HIF-1α to be elevated under all hypoxic conditions and in all cell lines. Additionally, the protein expression profiles of GLUT1 and LDHA were found to be mostly elevated under hypoxic conditions, whereas GLUL protein expression levels were mostly down regulated.

HIF-1α stabilization in response to environmental factors like hypoxia contributes in many ways to a pro-growth glycolytic metabolic program, by synchronizing proliferation rates with O_2 availability [158]. On the one hand, HIF-1α seems to be a perfect drug target for hypoxic tumors, but on the other hand, despite the promise of HIF-1 inhibitors as anticancer agents, preclinical and clinical development of many agents have been halted because of safety or toxicity concerns [71]. HIF-1α is known to be an important contributor to the Warburg effect by inducing the expression of genes encoding glycolytic enzymes and glucose transporters [159], [160]. Therefore, my results are in line with previous observations, as I could show that the glucose transporter GLUT1 is upregulated during HIF-1α stabilization. Furthermore, HIF-1α also directly regulates the expression of the enzyme lactate dehydrogenase A (LDHA) and the monocarboxylate transporter 4 (MCT4) cell surface transporter, which mediates the efflux of lactate from the cell [161]. Promotion of lactate production by HIF-1α is a phenomenon, that is also reflected in my data set [162]. GLUT1 and LDHA are among the top-regulated targets suggesting that HIF-1α-induced upregulation of GLUT1 and LDHA contribute to the effective glycolytic production of lactic acid, a feature that has been suggested to promote survival in hypoxic settings [163]. Conversion of pyruvate to lactate and its removal by lactate transporters allows cancer cells to regenerate NAD^+ and maintain glycolytic flux in hypoxia [164]. These findings are consistent with prior studies reporting a substantial shift towards anaerobic glycolysis as the major metabolic feature of HIF-1α expressing cells. This indicates that glycolysis may be the preferred pathway used for energy production in hypoxic states. However, under conditions of unlimited nutrient resources, cells are also able to utilize a variety of metabolic processes, including OXPHOS to generate energy. Drugs that target glycolytic enzymes and transporters of glycolytic products, such as

GLUT1 and LDHA have been investigated in several preclinical studies and some, like the GLUT1 inhibitor Silibinin are been tested clinically [165], [166], [167]. However, no inhibitors of glycolysis have yet been approved as anticancer agents.

As described above, GLUT1 and LDHA, two of the three top regulated metabolism related proteins that I identified in my perturbation experiments, have been broadly explored in several studies and thus serve as a benchmark for my results. However, these lack novelty for further exploration. Therefore, I focused on exploring the rather unknown connection of GLUL and hypoxia.

Glutamate-ammonia ligase (GLUL), an enzyme which catalyzes the de novo synthesis of glutamine from glutamate and ammonia, was found to be significantly perturbed during hypoxia exposure in all cell lines. Glutamine, in principle a non-essential amino acid, belongs to a group of amino acids that are conditionally essential, particularly under catabolic stressed conditions in which glutamine consumption rises dramatically [168]. Glutamine is transported into cells through transporters, such as the ASCT2 transporter, that I found to be significantly associated with survival in breast cancer patients and further discussed in depth in the previous section of this Chapter [169]. Glutamine can be used for biosynthesis or be exported back out of the cell by antiporters in exchange for other amino acids such as leucine [54]. Overall, studies with tracer experiments have determined that at least 50% of non-essential amino acids used in protein synthesis by cancer cells in vitro, can be directly derived from glutamine [170]. Although the crucial role of glutamine metabolism in cancer cell lines is well established, it is less clear what role glutamine plays in tumors, where cells can face shortages of nutrients and oxygen [171]. I found the glutamine producing enzyme GLUL to be down regulated after exposure to hypoxia, indicating a reduced need for glutamine under hypoxic conditions. Further, I explored the connections between GLUL expression and clinicopathological characteristics of patients, using The Cancer Genome Atlas (TCGA) dataset. GLUL mRNA expression was found to be highest among all glutaminolysis related genes in the TCGA dataset and significantly higher expressed in the luminal breast cancer subtypes in comparison to the basal subtype. Furthermore, Kaplan-Meier analysis revealed a significant association of GLUL gene expression with both, OS and RFS. The most favorable overall and recurrence-free survival was represented by high GLUL expression, whereas low GLUL expression correlated with poor outcome. A significant association of lower GLUL expression with a higher T stage and vice versa was in line with these observations.

GLUL promotes glutamine production which can be used for anabolic processes such as synthesis of nucleotides and proteins. These building blocks are crucial for proliferation and the growth of cancer cells. My data reflects the general notion for the need of high glutamine levels in order to sustain cellular processes, as GLUL was found highly expressed in breast cancer patients and the association of high GLUL expression and favorable patient survival underlines this aspect.

In summary, combining all results, poor outcome was found for patients with high HIF-1α and low GLUL gene expression. GLUL mRNA expression levels were significantly elevated in the HIF-1α low patient subgroup, whereas low GLUL expression was associated with the HIF-1α high expressing patient subgroup. These results illustrate the association of survival and decreased GLUL expression under hypoxic conditions indicating a cellular metabolic switch from proliferation to "survival mode" and an inhibition of glutaminolysis during hypoxia. Cells undergo cell cycle arrest under conditions of severe hypoxia, but are capable of recovering if hypoxia is not prolonged [172]. Therefore, for future studies it would be highly interesting to explore GLUL and its association with hypoxic conditions in more depth and a possible role of GLUL as hypoxia marker in breast cancer patients.

Taken together, the maintenance of O_2 homeostasis is essential for the survival of most species. O_2 deprivation triggers complex adaptive responses at cellular, tissue and organismal levels to meet the metabolic and bioenergetic demands [173]. Most research concerning HIFs and their interaction with the metabolome has mostly focused on glycolysis. Revealing the effects of hypoxia using a broad panel of metabolism associated proteins has showed metabolic pathways beyond glycolysis that are important in cancer adaptation processes.

5.3 Concluding remarks and future directions

Cancer was recognized as a disease of altered metabolism nearly 100 years ago, but metabolic reprogramming has only recently been recognized as an essential hallmark of neoplasia. Mutations in metabolic enzymes can drive tumorigenesis, more often however cancer metabolism is transformed by altered abundance and activity of the metabolic enzymes [174]. While many of the underlying causes of human disease occur at genetic and epigenetic levels, drug response and disease pathophysiology are driven by cellular phenotypes that in turn are regulated at the translational protein level.

During the recent years, reverse phase protein arrays (RPPA) have emerged as a powerful high-throughput approach for targeted proteomics [109], [121]. RPPA allows the quantification of protein expression profiles in large sample sets while requiring very low amounts of biological sample. Therefore, the RPPA platform was ideally suited for my analysis of clinical materials and biomarker discovery purposes [175], [176], [177].

With respect to the current focus on outcome-based therapy and precision medicine, the identification of novel therapeutic proteins and prognostic biomarkers is critical for future clinical patient stratification and drug discovery.

In the present study, I applied RPPA-based functional proteomics to a large number of patient samples from a multicenter prospective cohort, to evaluate the relationship between metabolism-associated protein expression profiles and clinicopathological characteristics. Clustering results, as well as individual protein expression patterns were associated with clinical data. The results showed metabolism associated proteins linked to breast cancer progression and metabolic clusters of breast cancer, characterized by differences at the proteomic level. Particularly, proteins mapping to the ‘diffuse’ cluster, were found to be associated with poor prognosis. Moreover, the results highlight the importance of SHMT2 and ASCT2 protein expression as independent prognostic factors and potential prognostic biomarkers for breast cancer patients, as their high protein expression is associated with poor outcome.

The results confirm the reported heterogeneity of breast tumors at a functional proteomic level and dissect the relationship between metabolism related proteins, pathological features and patient survival.

Although my project revealed the clinical significance of SHMT2 and ASCT2 in breast cancer, some limitations warrant further investigation. For instance, the functional roles of SHMT2 and ASCT2. Furthermore, an investigation of an independent cohort is needed to validate the findings. Since a long-term follow-up of the patient cohort is conducted, continuous monitoring of the prognostic power of the achieved results would be a suitable consideration.

In the second part of my study, I demonstrated that breast cancer cell lines regulate their metabolic protein levels in heterogeneous ways during oxygen deprived conditions. My results showed a significant regulation of a minor amount of proteins in all cell lines and conditions tested, rather than a complete pathway response. Among the top-regulated protein targets were known effectors of HIF-1α, such as GLUT1 and LDHA. Also, the novel discovery of a significant regulation of GLUL in all cell lines and perturbation experiments was observed. Particularly, GLUL showed an inverse correlation of protein expression compared to HIF-1α and was further found to be associated with survival in breast cancer patients.

Although first insights into the hypoxic response of metabolism related targets was revealed, further investigations are needed to validate the findings. A more comprehensive investigation of GLUL and its regulation e.g. in glutamine-deprived conditions might foster new insights. The behavior of GLUL overexpressing cells to hypoxic conditions could lead to a better understanding of the role of glutaminolysis in an oxygen deprived microenvironment.

In general, revealing new markers of HIF metabolism could lead to a better understanding of the phenotype and may enable more successful diagnosis and prognosis of patients with hypoxic tumors. Screening tumor extracts for relevant hypoxic signatures could thus be a first step towards identifying appropriate stratification regimes. Therefore, exploring GLUL and its association with hypoxic conditions in future studies and to investigate a possible role of GLUL as a hypoxia marker in breast cancer patients, could be a promising approach.

References

1. Hanahan D, Weinberg RA. The Hallmarks of Cancer. Cell. 2000;100:57–70.

2. Hanahan D, Weinberg RA. Hallmarks of cancer: the next generation. Cell. 2011;144:646–74.

3. Gatenby RA, Gillies RJ. A microenvironmental model of carcinogenesis. Nat Rev Cancer. 2008;8:56–61.

4. Siegel RL, Miller KD, Jemal A. Cancer Statistics, 2017. CA Cancer J Clin. 2017;67:7–30.

5. Curtis C, Shah SP, Chin SF, Turashvili G, Rueda OM, Dunning MJ, et al. The genomic and transcriptomic architecture of 2,000 breast tumours reveals novel subgroups. Nature. 2012;486:346–52.

6. Weigelt B, Reis-Filho JS. Histological and molecular types of breast cancer: is there a unifying taxonomy? Nat Rev Clin Oncol. 2009;6:718–30.

7. Ferlay J, Soerjomataram I, Dikshit R, Eser S, Mathers C, Rebelo M, et al. Cancer incidence and mortality worldwide: sources, methods and major patterns in GLOBOCAN 2012. Int J Cancer. 2015;136:E359-386.

8. Bertos NR, Park M. Breast cancer - one term, many entities? J Clin Invest. 2011;121:3789–96.

9. Pinder SE, Ellis IO. The diagnosis and management of pre-invasive breast disease: ductal carcinoma in situ (DCIS) and atypical ductal hyperplasia (ADH)--current definitions and classification. Breast Cancer Res BCR. 2003;5:254–7.

10. Institute of Medicine (US) and National Research Council (US) Committee on New Approaches to Early Detection and Diagnosis of Breast Cancer. Saving Women's Lives: Strategies for Improving Breast Cancer Detection and Diagnosis. Washington (DC): National Academies Press (US); 2005. http://www.ncbi.nlm.nih.gov/books/NBK22315/. Accessed 15 May 2017.

11. Blamey RW, Wilson AR, Patnick J. ABC of breast diseases: screening for breast cancer. BMJ. 2000;321:689–93.

12. Goldhirsch A, Wood WC, Coates AS, Gelber RD, Thürlimann B, Senn H-J, et al. Strategies for subtypes—dealing with the diversity of breast cancer: highlights of the St Gallen International Expert Consensus on the Primary Therapy of Early Breast Cancer 2011. Ann Oncol. 2011;22:1736–47.

13. Robertson JF, Dixon AR, Nicholson RI, Ellis IO, Elston CW, Blamey RW. Confirmation of a prognostic index for patients with metastatic breast cancer treated by endocrine therapy. Breast Cancer Res Treat. 1992;22:221–7.

14. Robertson JF, Bates K, Pearson D, Blamey RW, Nicholson RI. Comparison of two oestrogen receptor assays in the prediction of the clinical course of patients with advanced breast cancer. Br J Cancer. 1992;65:727–30.

15. Ravdin PM, Chamness GC. The c-erbB-2 proto-oncogene as a prognostic and predictive marker in breast cancer: a paradigm for the development of other macromolecular markers--a review. Gene. 1995;159:19–27.

16. Junttila TT, Akita RW, Parsons K, Fields C, Lewis Phillips GD, Friedman LS, et al. Ligand-independent HER2/HER3/PI3K complex is disrupted by trastuzumab and is effectively inhibited by the PI3K inhibitor GDC-0941. Cancer Cell. 2009;15:429–40.

17. Wittekind C, Compton CC, Greene FL, Sobin LH. TNM residual tumor classification revisited. Cancer. 2002;94:2511–6.

18. van de Vijver MJ, He YD, van't Veer LJ, Dai H, Hart AAM, Voskuil DW, et al. A gene-expression signature as a predictor of survival in breast cancer. N Engl J Med. 2002;347:1999–2009.

19. Sørlie T, Perou CM, Tibshirani R, Aas T, Geisler S, Johnsen H, et al. Gene expression patterns of breast carcinomas distinguish tumor subclasses with clinical implications. Proc Natl Acad Sci U S A. 2001;98:10869–74.

20. Cancer Genome Atlas N. Comprehensive molecular portraits of human breast tumours. Nature. 2012;490:61–70.

21. Bayraktar S, Royce M, Stork-Sloots L, de Snoo F, Glück S. Molecular subtyping predicts pathologic tumor response in early-stage breast cancer treated with neoadjuvant docetaxel plus capecitabine with or without trastuzumab chemotherapy. Med Oncol Northwood Lond Engl. 2014;31:163.

22. Bastien RRL, Rodríguez-Lescure Á, Ebbert MTW, Prat A, Munárriz B, Rowe L, et al. PAM50 breast cancer subtyping by RT-qPCR and concordance with standard clinical molecular markers. BMC Med Genomics. 2012;5:44.

23. Dowsett M, Sestak I, Lopez-Knowles E, Sidhu K, Dunbier AK, Cowens JW, et al. Comparison of PAM50 risk of recurrence score with oncotype DX and IHC4 for predicting risk of distant recurrence after endocrine therapy. J Clin Oncol Off J Am Soc Clin Oncol. 2013;31:2783–90.

24. Eiermann W, Rezai M, Kümmel S, Kühn T, Warm M, Friedrichs K, et al. The 21-gene recurrence score assay impacts adjuvant therapy recommendations for ER-positive, node-negative and node-positive early breast cancer resulting in a risk-adapted change in chemotherapy use. Ann Oncol Off J Eur Soc Med Oncol. 2013;24:618–24.

25. Ein-Dor L, Kela I, Getz G, Givol D, Domany E. Outcome signature genes in breast cancer: is there a unique set? Bioinforma Oxf Engl. 2005;21:171–8.

26. Sims AH, Howell A, Howell SJ, Clarke RB. Origins of breast cancer subtypes and therapeutic implications. Nat Clin Pract Oncol. 2007;4:516–25.

27. Brenton JD, Carey LA, Ahmed AA, Caldas C. Molecular classification and molecular forecasting of breast cancer: ready for clinical application? J Clin Oncol Off J Am Soc Clin Oncol. 2005;23:7350–60.

28. Harris LN, Ismaila N, McShane LM, Andre F, Collyar DE, Gonzalez-Angulo AM, et al. Use of Biomarkers to Guide Decisions on Adjuvant Systemic Therapy for Women With Early-Stage Invasive Breast Cancer: American Society of Clinical Oncology Clinical Practice Guideline. J Clin Oncol Off J Am Soc Clin Oncol. 2016;34:1134–50.

29. Niederhuber JE, Armitage JO, Doroshow JH, Kastan MB, Tepper JE, Abeloff MD. Abeloff's clinical oncology. Fifth edition. Philadelphia, Pennsylvania: Elsevier; 2014.

30. Senkus E, Kyriakides S, Ohno S, Penault-Llorca F, Poortmans P, Rutgers E, et al. Primary breast cancer: ESMO Clinical Practice Guidelines for diagnosis, treatment and follow-up. Ann Oncol. 2015;26 suppl_5:v8–30.

31. Herbst RS, Soria J-C, Kowanetz M, Fine GD, Hamid O, Gordon MS, et al. Predictive correlates of response to the anti-PD-L1 antibody MPDL3280A in cancer patients. Nature. 2014;515:563–7.

32. Feng Q, Zhang Z, Shea MJ, Creighton CJ, Coarfa C, Hilsenbeck SG, et al. An epigenomic approach to therapy for tamoxifen-resistant breast cancer. Cell Res. 2014;24:809–19.

33. Warburg O, Posener K, Negelein E. Ueber den Stoffwechsel der Tumoren. Biochem Z. 1924;:319–44.

34. Warburg O. On the origin of cancer cells. Science. 1956;123:309–14.

35. Ward PS, Thompson CB. Metabolic reprogramming: a cancer hallmark even warburg did not anticipate. Cancer Cell. 2012;21:297–308.

36. Kroemer G, Pouyssegur J. Tumor cell metabolism: cancer's Achilles' heel. Cancer Cell. 2008;13:472–82.

37. Cantor JR, Sabatini DM. Cancer cell metabolism: one hallmark, many faces. Cancer Discov. 2012;2:881–98.

38. Vander Heiden MG. Exploiting tumor metabolism: challenges for clinical translation. J Clin Invest. 2013;123:3648–51.

39. Warburg O, Wind F, Negelein E. THE METABOLISM OF TUMORS IN THE BODY. J Gen Physiol. 1927;8:519–30.

40. Vander Heiden MG, Cantley LC, Thompson CB. Understanding the Warburg effect: the metabolic requirements of cell proliferation. Science. 2009;324:1029–33.

41. Gatenby RA, Gawlinski ET, Gmitro AF, Kaylor B, Gillies RJ. Acid-mediated tumor invasion: a multidisciplinary study. Cancer Res. 2006;66:5216–23.

42. Fantin VR, St-Pierre J, Leder P. Attenuation of LDH-A expression uncovers a link between glycolysis, mitochondrial physiology, and tumor maintenance. Cancer Cell. 2006;9:425–34.

43. Lunt SY, Vander Heiden MG. Aerobic glycolysis: meeting the metabolic requirements of cell proliferation. Annu Rev Cell Dev Biol. 2011;27:441–64.

44. Sai KKS, Zachar Z, Bingham PM, Mintz A. Metabolic PET Imaging in Oncology. Am J Roentgenol. 2017;:1–7.

45. Moreno-Sánchez R, Rodríguez-Enríquez S, Marín-Hernández A, Saavedra E. Energy metabolism in tumor cells. FEBS J. 2007;274:1393–418.

46. DeBerardinis RJ, Lum JJ, Hatzivassiliou G, Thompson CB. The biology of cancer: metabolic reprogramming fuels cell growth and proliferation. Cell Metab. 2008;7:11–20.

47. Curi R, Lagranha CJ, Doi SQ, Sellitti DF, Procopio J, Pithon-Curi TC, et al. Molecular mechanisms of glutamine action. J Cell Physiol. 2005;204:392–401.

48. DeBerardinis RJ, Mancuso A, Daikhin E, Nissim I, Yudkoff M, Wehrli S, et al. Beyond aerobic glycolysis: transformed cells can engage in glutamine metabolism that exceeds the requirement for protein and nucleotide synthesis. Proc Natl Acad Sci U S A. 2007;104:19345–50.

49. Stein WH, Moore S. The free amino acids of human blood plasma. J Biol Chem. 1954;211:915–26.

50. Young VR, Ajami AM. Glutamine: The Emperor or His Clothes? J Nutr. 2001;131:2449S–2459S.

51. Wise DR, Thompson CB. Glutamine addiction: a new therapeutic target in cancer. Trends Biochem Sci. 2010;35:427–33.

52. Phang JM, Liu W, Hancock C, Christian KJ. The proline regulatory axis and cancer. Front Oncol. 2012;2:60.

53. Cendan JC, Topping DL, Pruitt J, Snowdy S, Copeland EM, Lind DS. Inflammatory mediators stimulate arginine transport and arginine-derived nitric oxide production in a murine breast cancer cell line. J Surg Res. 1996;60:284–8.

54. Nicklin P, Bergman P, Zhang B, Triantafellow E, Wang H, Nyfeler B, et al. Bidirectional transport of amino acids regulates mTOR and autophagy. Cell. 2009;136:521–34.

55. Pingitore P, Pochini L, Scalise M, Galluccio M, Hedfalk K, Indiveri C. Large scale production of the active human ASCT2 (SLC1A5) transporter in Pichia pastoris--functional and kinetic asymmetry revealed in proteoliposomes. Biochim Biophys Acta. 2013;1828:2238–46.

56. Szeliga M, Obara-Michlewska M. Glutamine in neoplastic cells: focus on the expression and roles of glutaminases. Neurochem Int. 2009;55:71–5.

57. Vander Heiden MG. Targeting cancer metabolism: a therapeutic window opens. Nat Rev Drug Discov. 2011;10:671–84.

58. Yuneva M, Zamboni N, Oefner P, Sachidanandam R, Lazebnik Y. Deficiency in glutamine but not glucose induces MYC-dependent apoptosis in human cells. J Cell Biol. 2007;178:93–105.

59. DeBerardinis RJ, Cheng T. Q's next: the diverse functions of glutamine in metabolism, cell biology and cancer. Oncogene. 2010;29:313–24.

60. Wullschleger S, Loewith R, Hall MN. TOR signaling in growth and metabolism. Cell. 2006;124:471–84.

61. Salvo ML di, Contestabile R, Paiardini A, Maras B. Glycine consumption and mitochondrial serine hydroxymethyltransferase in cancer cells: The heme connection. Med Hypotheses. 2013;80:633–6.

62. Jain M, Nilsson R, Sharma S, Madhusudhan N, Kitami T, Souza AL, et al. Metabolite profiling identifies a key role for glycine in rapid cancer cell proliferation. Science. 2012;336:1040–4.

63. Pollari S, Käkönen S-M, Edgren H, Wolf M, Kohonen P, Sara H, et al. Enhanced serine production by bone metastatic breast cancer cells stimulates osteoclastogenesis. Breast Cancer Res Treat. 2011;125:421–30.

64. Possemato R, Marks KM, Shaul YD, Pacold ME, Kim D, Birsoy K, et al. Functional genomics reveal that the serine synthesis pathway is essential in breast cancer. Nature. 2011;476:346–50.

65. Locasale JW, Grassian AR, Melman T, Lyssiotis CA, Mattaini KR, Bass AJ, et al. Phosphoglycerate dehydrogenase diverts glycolytic flux and contributes to oncogenesis. Nat Genet. 2011;43:869–74.

66. Maddocks ODK, Berkers CR, Mason SM, Zheng L, Blyth K, Gottlieb E, et al. Serine starvation induces stress and p53-dependent metabolic remodelling in cancer cells. Nature. 2013;493:542–6.

67. Labuschagne CF, van den Broek NJF, Mackay GM, Vousden KH, Maddocks ODK. Serine, but not glycine, supports one-carbon metabolism and proliferation of cancer cells. Cell Rep. 2014;7:1248–58.

68. Gautier EL, Westerterp M, Bhagwat N, Cremers S, Shih A, Abdel-Wahab O, et al. HDL and Glut1 inhibition reverse a hypermetabolic state in mouse models of myeloproliferative disorders. J Exp Med. 2013;210:339–53.

69. Yun J, Rago C, Cheong I, Pagliarini R, Angenendt P, Rajagopalan H, et al. Glucose deprivation contributes to the development of KRAS pathway mutations in tumor cells. Science. 2009;325:1555–9.

70. Michelakis ED, Webster L, Mackey JR. Dichloroacetate (DCA) as a potential metabolic-targeting therapy for cancer. Br J Cancer. 2008;99:989–94.

71. Wilson WR, Hay MP. Targeting hypoxia in cancer therapy. Nat Rev Cancer. 2011;11:393–410.

72. Engelman JA. Targeting PI3K signalling in cancer: opportunities, challenges and limitations. Nat Rev Cancer. 2009;9:550–62.

73. Brown NS, Bicknell R. Hypoxia and oxidative stress in breast cancer: Oxidative stress: its effects on the growth, metastatic potential and response to therapy of breast cancer. Breast Cancer Res BCR. 2001;3:323–7.

74. Wang J, Biedermann KA, Brown JM. Repair of DNA and chromosome breaks in cells exposed to SR 4233 under hypoxia or to ionizing radiation. Cancer Res. 1992;52:4473–7.

75. Bristow RG, Hill RP. Hypoxia and metabolism: Hypoxia, DNA repair and genetic instability. Nat Rev Cancer. 2008;8:180–92.

76. Dewhirst MW, Cao Y, Moeller B. Cycling hypoxia and free radicals regulate angiogenesis and radiotherapy response. Nat Rev Cancer. 2008;8:425–37.

77. Brahimi-Horn MC, Chiche J, Pouysségur J. Hypoxia and cancer. J Mol Med Berl Ger. 2007;85:1301–7.

78. Rzymski T, Harris AL. The unfolded protein response and integrated stress response to anoxia. Clin Cancer Res Off J Am Assoc Cancer Res. 2007;13:2537–40.

79. Vaupel P, Kallinowski F, Okunieff P. Blood Flow, Oxygen and Nutrient Supply, and Metabolic Microenvironment of Human Tumors: A Review. Cancer Res. 1989;49:6449–65.

80. Wang GL, Semenza GL. Purification and characterization of hypoxia-inducible factor 1. J Biol Chem. 1995;270:1230–7.

81. Bruick RK, McKnight SL. A conserved family of prolyl-4-hydroxylases that modify HIF. Science. 2001;294:1337–40.

82. Ivan M, Kondo K, Yang H, Kim W, Valiando J, Ohh M, et al. HIFalpha targeted for VHL-mediated destruction by proline hydroxylation: implications for O2 sensing. Science. 2001;292:464–8.

83. Webb JD, Coleman ML, Pugh CW. Hypoxia, hypoxia-inducible factors (HIF), HIF hydroxylases and oxygen sensing. Cell Mol Life Sci CMLS. 2009;66:3539–54.

84. Vaupel P, Mayer A. Hypoxia in cancer: significance and impact on clinical outcome. Cancer Metastasis Rev. 2007;26:225–39.

85. Semenza GL. Regulation of oxygen homeostasis by hypoxia-inducible factor 1. Physiol Bethesda Md. 2009;24:97–106.

86. Ramakrishnan SK, Shah YM. Role of Intestinal HIF-2α in Health and Disease. Annu Rev Physiol. 2016;78:301–25.

87. Keith B, Johnson RS, Simon MC. HIF1α and HIF2α: sibling rivalry in hypoxic tumor growth and progression. Nat Rev Cancer. 2011;12:9–22.

88. Qing G, Simon MC. Hypoxia inducible factor-2alpha: a critical mediator of aggressive tumor phenotypes. Curr Opin Genet Dev. 2009;19:60–6.

89. Duan C. Hypoxia-inducible factor 3 biology: complexities and emerging themes. Am J Physiol Cell Physiol. 2016;310:C260-269.

90. Zhong H, De Marzo AM, Laughner E, Lim M, Hilton DA, Zagzag D, et al. Overexpression of hypoxia-inducible factor 1alpha in common human cancers and their metastases. Cancer Res. 1999;59:5830–5.

91. Talks KL, Turley H, Gatter KC, Maxwell PH, Pugh CW, Ratcliffe PJ, et al. The expression and distribution of the hypoxia-inducible factors HIF-1alpha and HIF-2alpha in normal human tissues, cancers, and tumor-associated macrophages. Am J Pathol. 2000;157:411–21.

92. Bárdos JI, Ashcroft M. Hypoxia-inducible factor-1 and oncogenic signalling. BioEssays News Rev Mol Cell Dev Biol. 2004;26:262–9.

93. Harris AL. Hypoxia--a key regulatory factor in tumour growth. Nat Rev Cancer. 2002;2:38–47.

94. Rofstad EK, Galappathi K, Mathiesen B, Ruud E-BM. Fluctuating and diffusion-limited hypoxia in hypoxia-induced metastasis. Clin Cancer Res Off J Am Assoc Cancer Res. 2007;13:1971–8.

95. Forsythe JA, Jiang BH, Iyer NV, Agani F, Leung SW, Koos RD, et al. Activation of vascular endothelial growth factor gene transcription by hypoxia-inducible factor 1. Mol Cell Biol. 1996;16:4604–13.

96. Caldwell CC, Kojima H, Lukashev D, Armstrong J, Farber M, Apasov SG, et al. Differential effects of physiologically relevant hypoxic conditions on T lymphocyte development and effector functions. J Immunol Baltim Md 1950. 2001;167:6140–9.

97. Chiche J, Brahimi-Horn MC, Pouysségur J. Tumour hypoxia induces a metabolic shift causing acidosis: a common feature in cancer. J Cell Mol Med. 2010;14:771–94.

98. Minchenko A, Leshchinsky I, Opentanova I, Sang N, Srinivas V, Armstead V, et al. Hypoxia-inducible factor-1-mediated expression of the 6-phosphofructo-2-kinase/fructose-2,6-bisphosphatase-3 (PFKFB3) gene. Its possible role in the Warburg effect. J Biol Chem. 2002;277:6183–7.

99. Chan DA, Giaccia AJ. Hypoxia, gene expression, and metastasis. Cancer Metastasis Rev. 2007;26:333–9.

100. Schindl M, Schoppmann SF, Samonigg H, Hausmaninger H, Kwasny W, Gnant M, et al. Overexpression of hypoxia-inducible factor 1alpha is associated with an unfavorable prognosis in lymph node-positive breast cancer. Clin Cancer Res Off J Am Assoc Cancer Res. 2002;8:1831–7.

101. Semenza GL. Defining the role of hypoxia-inducible factor 1 in cancer biology and therapeutics. Oncogene. 2010;29:625–34.

102. Milosevic M, Fyles A, Hedley D, Hill R. The human tumor microenvironment: invasive (needle) measurement of oxygen and interstitial fluid pressure. Semin Radiat Oncol. 2004;14:249–58.

103. Busk M, Horsman MR, Jakobsen S, Bussink J, van der Kogel A, Overgaard J. Cellular uptake of PET tracers of glucose metabolism and hypoxia and their linkage. Eur J Nucl Med Mol Imaging. 2008;35:2294–303.

104. Winter SC, Buffa FM, Silva P, Miller C, Valentine HR, Turley H, et al. Relation of a hypoxia metagene derived from head and neck cancer to prognosis of multiple cancers. Cancer Res. 2007;67:3441–9.

105. Chi J-T, Wang Z, Nuyten DSA, Rodriguez EH, Schaner ME, Salim A, et al. Gene expression programs in response to hypoxia: cell type specificity and prognostic significance in human cancers. PLoS Med. 2006;3:e47.

106. Rapisarda A, Melillo G. Overcoming disappointing results with antiangiogenic therapy by targeting hypoxia. Nat Rev Clin Oncol. 2012;9:378–90.

107. Ekins RP. Multi-analyte immunoassay. J Pharm Biomed Anal. 1989;7:155–68.

108. Ekins RP, Chu FW. Multianalyte microspot immunoassay--microanalytical "compact disk" of the future. Clin Chem. 1991;37:1955–67.

109. Paweletz CP, Charboneau L, Bichsel VE, Simone NL, Chen T, Gillespie JW, et al. Reverse phase protein microarrays which capture disease progression show activation of pro-survival pathways at the cancer invasion front. Oncogene. 2001;20:1981–9.

110. Liotta LA, Espina V, Mehta AI, Calvert V, Rosenblatt K, Geho D, et al. Protein microarrays: Meeting analytical challenges for clinical applications. Cancer Cell. 2003;3:317–25.

111. Agarwal R, Gonzalez-Angulo A-M, Myhre S, Carey M, Lee J-S, Overgaard J, et al. Integrative Analysis of Cyclin Protein Levels Identifies Cyclin B1 as a Classifier and Predictor of Outcomes in Breast Cancer. Clin Cancer Res. 2009;15:3654–62.

112. Nishizuka S, Charboneau L, Young L, Major S, Reinhold WC, Waltham M, et al. Proteomic profiling of the NCI-60 cancer cell lines using new high-density reverse-phase lysate microarrays. Proc Natl Acad Sci. 2003;100:14229–34.

113. Srivastava M, Eidelman O, Zhang J, Paweletz C, Caohuy H, Yang Q, et al. Digitoxin mimics gene therapy with CFTR and suppresses hypersecretion of IL-8 from cystic fibrosis lung epithelial cells. Proc Natl Acad Sci U S A. 2004;101:7693–8.

114. Grote T, Siwak DR, Fritsche HA, Joy C, Mills GB, Simeone D, et al. Validation of reverse phase protein array for practical screening of potential biomarkers in serum and plasma: accurate detection of CA19-9 levels in pancreatic cancer. Proteomics. 2008;8:3051–60.

115. Kornblau SM, Singh N, Qiu Y, Chen W, Zhang N, Coombes KR. Highly Phosphorylated FOXO3A Is an Adverse Prognostic Factor in Acute Myeloid Leukemia. Clin Cancer Res. 2010;16:1865–74.

116. Boin A, Couvelard A, Couderc C, Brito I, Filipescu D, Kalamarides M, et al. Proteomic screening identifies a YAP-driven signaling network linked to tumor cell proliferation in human schwannomas. Neuro Oncol. 2014. doi:10.1093/neuonc/nou020.

117. Srivastava M, Eidelman O, Torosyan Y, Jozwik C, Mannon RB, Pollard HB. Elevated Expression Levels of ANXA11, Integrins β3 and α3, and TNFα Contribute to a Candidate Proteomic Signature in Urine for Kidney Allograft Rejection. Proteomics Clin Appl. 2011;5:311–21.

118. Rapkiewicz A, Espina V, Zujewski JA, Lebowitz PF, Filie A, Wulfkuhle J, et al. The needle in the haystack: application of breast fine-needle aspirate samples to quantitative protein microarray technology. Cancer. 2007;111:173–84.

119. Pawlak M, Schick E, Bopp MA, Schneider MJ, Oroszlan P, Ehrat M. Zeptosens' protein microarrays: a novel high performance microarray platform for low abundance protein analysis. Proteomics. 2002;2:383–93.

120. Shi T, Fillmore TL, Sun X, Zhao R, Schepmoes AA, Hossain M, et al. Antibody-free, targeted mass-spectrometric approach for quantification of proteins at low picogram per milliliter levels in human plasma/serum. Proc Natl Acad Sci. 2012;109:15395–400.

121. Akbani R, Baker KF, Carragher N, Goldstein T, de Koning L, Korf U, et al. Realizing the promise of reverse phase protein arrays for clinical, translational and basic research : a workshop report. Mol Cell Proteomics. 2014. doi:10.1074/mcp.O113.034918.

122. Loebke C, Sueltmann H, Schmidt C, Henjes F, Wiemann S, Poustka A, et al. Infrared-based protein detection arrays for quantitative proteomics. PROTEOMICS. 2007;7:558–64.

123. Mannsperger HA, Gade S, Henjes F, Beissbarth T, Korf U. RPPanalyzer: Analysis of reverse-phase protein array data. Bioinforma Oxf Engl. 2010;26:2202–3.

124. von der Heyde S, Sonntag J, Kaschek D, Bender C, Bues J, Wachter A, et al. RPPanalyzer Toolbox: An improved R package for analysis of reverse phase protein array data. Biotechniques. 2014;57:125–35.

125. Henjes F, Bender C, von der Heyde S, Braun L, Mannsperger HA, Schmidt C, et al. Strong EGFR signaling in cell line models of ERBB2-amplified breast cancer attenuates response towards ERBB2-targeting drugs. Oncogenesis. 2012;1:e16.

126. Sobin LH, Gospodarowicz MK, Wittekind C. TNM Classification of Malignant Tumours. New York, NY: John Wiley & Sons; 2011. http://nbn-resolving.de/urn:nbn:de:101:1-201411168422. Accessed 14 Feb 2017.

127. Minckwitz G von, Untch M, Blohmer J-U, Costa SD, Eidtmann H, Fasching PA, et al. Definition and Impact of Pathologic Complete Response on Prognosis After Neoadjuvant Chemotherapy in Various Intrinsic Breast Cancer Subtypes. J Clin Oncol. 2012;30:1796–804.

128. Hudis CA, Barlow WE, Costantino JP, Gray RJ, Pritchard KI, Chapman J-AW, et al. Proposal for standardized definitions for efficacy end points in adjuvant breast cancer trials: the STEEP system. J Clin Oncol Off J Am Soc Clin Oncol. 2007;25:2127–32.

129. R Core Team. R: A Language and Environment for Statistical Computing. 2013. https://www.r-project.org/. Accessed 12 Dec 2016.

130. Szklarczyk D, Franceschini A, Wyder S, Forslund K, Heller D, Huerta-Cepas J, et al. STRING v10: protein-protein interaction networks, integrated over the tree of life. Nucleic Acids Res. 2015;43 Database issue:D447-452.

131. Galili T. dendextend: an R package for visualizing, adjusting and comparing trees of hierarchical clustering. Bioinforma Oxf Engl. 2015;31:3718–20.

132. Harrington DP, Fleming TR. A class of rank test procedures for censored survival data. Biometrika. 1982;69:553–66.

133. Modeling Survival Data: Extending the Cox Model | Terry M. Therneau | Springer. http://www.springer.com/de/book/9780387987842. Accessed 9 Dec 2016.

134. Benjamini Y, Hochberg Y. Controlling the False Discovery Rate: A Practical and Powerful Approach to Multiple Testing. J R Stat Soc Ser B Methodol. 1995;57:289–300.

135. Cook RD. Detection of Influential Observation in Linear Regression. Technometrics. 1977;19:15–8.

136. Cook RD. Influential Observations in Linear Regression. J Am Stat Assoc. 1979;74:169–74.

137. Gao J, Aksoy BA, Dogrusoz U, Dresdner G, Gross B, Sumer SO, et al. Integrative analysis of complex cancer genomics and clinical profiles using the cBioPortal. Sci Signal. 2013;6:pl1.

138. Cerami E, Gao J, Dogrusoz U, Gross BE, Sumer SO, Aksoy BA, et al. The cBio Cancer Genomics Portal: An Open Platform for Exploring Multidimensional Cancer Genomics Data. Cancer Discov. 2012;2:401–4.

139. Breitling R, Armengaud P, Amtmann A, Herzyk P. Rank products: a simple, yet powerful, new method to detect differentially regulated genes in replicated microarray experiments. FEBS Lett. 2004;573:83–92.

140. Mertins P, Mani DR, Ruggles KV, Gillette MA, Clauser KR, Wang P, et al. Proteogenomics connects somatic mutations to signalling in breast cancer. Nature. 2016;534:55–62.

141. Myhre S, Lingjærde O-C, Hennessy BT, Aure MR, Carey MS, Alsner J, et al. Influence of DNA copy number and mRNA levels on the expression of breast cancer related proteins. Mol Oncol. 2013;7:704–18.

142. Mullen AR, Wheaton WW, Jin ES, Chen P-H, Sullivan LB, Cheng T, et al. Reductive carboxylation supports growth in tumour cells with defective mitochondria. Nature. 2011;481:385–8.

143. Dolfi SC, Chan LL, Qiu J, Tedeschi PM, Bertino JR, Hirshfield KM, et al. The metabolic demands of cancer cells are coupled to their size and protein synthesis rates. Cancer Metab. 2013;1:20.

144. Ren P, Yue M, Xiao D, Xiu R, Gan L, Liu H, et al. ATF4 and N-Myc coordinate glutamine metabolism in MYCN-amplified neuroblastoma cells through ASCT2 activation. J Pathol. 2015;235:90–100.

145. Huang F, Zhao Y, Zhao J, Wu S, Jiang Y, Ma H, et al. Upregulated SLC1A5 promotes cell growth and survival in colorectal cancer. Int J Clin Exp Pathol. 2014;7:6006–14.

146. Wang Q, Hardie RA, Hoy AJ, van Geldermalsen M, Gao D, Fazli L, et al. Targeting ASCT2-mediated glutamine uptake blocks prostate cancer growth and tumour development. J Pathol. 2015;236:278–89.

147. Liu Y, Yang L, An H, Chang Y, Zhang W, Zhu Y, et al. High expression of Solute Carrier Family 1, member 5 (SLC1A5) is associated with poor prognosis in clear-cell renal cell carcinoma. Sci Rep. 2015;5:16954.

148. Shimizu K, Kaira K, Tomizawa Y, Sunaga N, Kawashima O, Oriuchi N, et al. ASC amino-acid transporter 2 (ASCT2) as a novel prognostic marker in non-small cell lung cancer. Br J Cancer. 2014;110:2030–9.

149. Fuchs BC, Bode BP. Amino acid transporters ASCT2 and LAT1 in cancer: partners in crime? Semin Cancer Biol. 2005;15:254–66.

150. Adeva MM, Souto G, Blanco N, Donapetry C. Ammonium metabolism in humans. Metabolism. 2012;61:1495–511.

151. Marin M, Lavillette D, Kelly SM, Kabat D. N-linked glycosylation and sequence changes in a critical negative control region of the ASCT1 and ASCT2 neutral amino acid transporters determine their retroviral receptor functions. J Virol. 2003;77:2936–45.

152. Nakaya M, Xiao Y, Zhou X, Chang J-H, Chang M, Cheng X, et al. Inflammatory T cell responses rely on amino acid transporter ASCT2 facilitation of glutamine uptake and mTORC1 kinase activation. Immunity. 2014;40:692–705.

153. Wang Q, Beaumont KA, Otte NJ, Font J, Bailey CG, van Geldermalsen M, et al. Targeting glutamine transport to suppress melanoma cell growth. Int J Cancer. 2014;135:1060–71.

154. Willems L, Jacque N, Jacquel A, Neveux N, Maciel TT, Lambert M, et al. Inhibiting glutamine uptake represents an attractive new strategy for treating acute myeloid leukemia. Blood. 2013;122:3521–32.

155. Sitter B, Bathen TF, Singstad TE, Fjøsne HE, Lundgren S, Halgunset J, et al. Quantification of metabolites in breast cancer patients with different clinical prognosis using HR MAS MR spectroscopy. NMR Biomed. 2010;23:424–31.

156. Pavlides S, Whitaker-Menezes D, Castello-Cros R, Flomenberg N, Witkiewicz AK, Frank PG, et al. The reverse Warburg effect: aerobic glycolysis in cancer associated fibroblasts and the tumor stroma. Cell Cycle Georget Tex. 2009;8:3984–4001.

157. Fiaschi T, Marini A, Giannoni E, Taddei ML, Gandellini P, De Donatis A, et al. Reciprocal metabolic reprogramming through lactate shuttle coordinately influences tumor-stroma interplay. Cancer Res. 2012;72:5130–40.

158. Semenza GL. HIF-1 mediates metabolic responses to intratumoral hypoxia and oncogenic mutations. J Clin Invest. 2013;123:3664–71.

159. Iyer NV, Kotch LE, Agani F, Leung SW, Laughner E, Wenger RH, et al. Cellular and developmental control of O2 homeostasis by hypoxia-inducible factor 1 alpha. Genes Dev. 1998;12:149–62.

160. Semenza GL, Jiang BH, Leung SW, Passantino R, Concordet JP, Maire P, et al. Hypoxia response elements in the aldolase A, enolase 1, and lactate dehydrogenase A gene promoters contain essential binding sites for hypoxia-inducible factor 1. J Biol Chem. 1996;271:32529–37.

161. Doherty JR, Cleveland JL. Targeting lactate metabolism for cancer therapeutics. J Clin Invest. 2013;123:3685–92.

162. Le A, Cooper CR, Gouw AM, Dinavahi R, Maitra A, Deck LM, et al. Inhibition of lactate dehydrogenase A induces oxidative stress and inhibits tumor progression. Proc Natl Acad Sci U S A. 2010;107:2037–42.

163. Kim J, Tchernyshyov I, Semenza GL, Dang CV. HIF-1-mediated expression of pyruvate dehydrogenase kinase: a metabolic switch required for cellular adaptation to hypoxia. Cell Metab. 2006;3:177–85.

164. Feron O. Pyruvate into lactate and back: from the Warburg effect to symbiotic energy fuel exchange in cancer cells. Radiother Oncol J Eur Soc Ther Radiol Oncol. 2009;92:329–33.

165. Galluzzi L, Kepp O, Heiden MG, Kroemer G. Metabolic targets for cancer therapy. Nat Rev Drug Discov. 2013;12:829–46.

166. Marchiq I, Pouysségur J. Hypoxia, cancer metabolism and the therapeutic benefit of targeting lactate/H(+) symporters. J Mol Med Berl Ger. 2016;94:155–71.

167. Deep G, Agarwal R. Targeting tumor microenvironment with silibinin: promise and potential for a translational cancer chemopreventive strategy. Curr Cancer Drug Targets. 2013;13:486–99.

168. Lacey JM, Wilmore DW. Is glutamine a conditionally essential amino acid? Nutr Rev. 1990;48:297–309.

169. Bhutia YD, Babu E, Ramachandran S, Ganapathy V. Amino Acid transporters in cancer and their relevance to "glutamine addiction": novel targets for the design of a new class of anticancer drugs. Cancer Res. 2015;75:1782–8.

170. Alberghina L, Gaglio D. Redox control of glutamine utilization in cancer. Cell Death Dis. 2014;5:e1561.

171. Mayers JR, Vander Heiden MG. Famine versus feast: understanding the metabolism of tumors in vivo. Trends Biochem Sci. 2015;40:130–40.

172. Gardner LB, Li Q, Park MS, Flanagan WM, Semenza GL, Dang CV. Hypoxia inhibits G1/S transition through regulation of p27 expression. J Biol Chem. 2001;276:7919–26.

173. Lee KE, Simon MC. SnapShot: Hypoxia-Inducible Factors. Cell. 2015;163:1288–1288.e1.

174. DeBerardinis RJ, Thompson CB. Cellular metabolism and disease: what do metabolic outliers teach us? Cell. 2012;148:1132–44.

175. Gonzalez-Angulo AM, Hennessy BT, Meric-Bernstam F, Sahin A, Liu W, Ju Z, et al. Functional proteomics can define prognosis and predict pathologic complete response in patients with breast cancer. Clin Proteomics. 2011;8:11.

176. Boyd ZS, Wu QJ, O'Brien C, Spoerke J, Savage H, Fielder PJ, et al. Proteomic analysis of breast cancer molecular subtypes and biomarkers of response to targeted kinase inhibitors using reverse-phase protein microarrays. Mol Cancer Ther. 2008;7:3695–706.

177. Frederick MJ, VanMeter AJ, Gadhikar MA, Henderson YC, Yao H, Pickering CC, et al. Phosphoproteomic Analysis of Signaling Pathways in Head and Neck Squamous Cell Carcinoma Patient Samples. Am J Pathol. 2011;178:548–71.

Appendices

Table S1 Relationship between clusters and clinical and pathological characteristics.

Please refer to the supplemented CD-ROM due to length of the table.

Table S2 Univariate Cox proportional hazard regression models of OS and RFS.

Target	HR	lower 95% CI	upper 95% CI	P	FDR
SHMT2	1.927	1.480	2.51	1.097E-06	4.060E-05
ASCT2	1.833	1.390	2.42	1.749E-05	0.000
GAPDH	1.480	1.119	1.96	0.006	0.075
SDHA	1.860	1.116	3.10	0.017	0.113
PKM2	1.414	1.056	1.89	0.020	0.113
FH	1.543	1.068	2.23	0.021	0.113
GLS	0.649	0.449	0.94	0.021	0.113
ASS1	1.342	1.022	1.76	0.035	0.160
ACC	0.618	0.377	1.01	0.057	0.197
CAD	1.689	0.977	2.92	0.060	0.197
GOT1	1.456	0.983	2.16	0.061	0.197
ARG2	1.519	0.968	2.38	0.069	0.197
GLUT1	1.213	0.985	1.49	0.069	0.197
LDHA	1.286	0.969	1.71	0.081	0.214
PCK2	0.810	0.636	1.03	0.087	0.214
PDH	1.567	0.918	2.67	0.100	0.231
PCK1	0.645	0.374	1.11	0.115	0.251
GLK	1.468	0.880	2.45	0.141	0.290
PSPH	0.795	0.560	1.13	0.199	0.384
IDH1	1.295	0.866	1.94	0.208	0.384
LAT1	1.194	0.867	1.65	0.278	0.489
LDHB	1.224	0.778	1.93	0.382	0.643
STARD10	0.867	0.609	1.24	0.432	0.653
ODC1	0.807	0.462	1.41	0.450	0.653
PKM1	0.850	0.553	1.31	0.459	0.653
SREBP1	1.132	0.815	1.57	0.459	0.653
PSAT1	1.154	0.729	1.83	0.541	0.741
NAGS	0.924	0.672	1.27	0.625	0.820
FASN	0.961	0.812	1.14	0.643	0.820
CPS1	1.059	0.809	1.39	0.676	0.834
GPT2	1.077	0.696	1.67	0.739	0.882
ASL	0.939	0.610	1.44	0.773	0.894
IDH2	0.960	0.692	1.33	0.810	0.908
SMS	0.968	0.651	1.44	0.873	0.950
PHGDH	1.026	0.658	1.60	0.909	0.961
Glud12	1.016	0.689	1.50	0.935	0.961
GLUL	0.995	0.789	1.26	0.968	0.968

Table S3 Correlations between key targets expression and patients and tumor characteristics.

Please refer to the supplemented CD-ROM due to length of the table.

Table S4 Univariate and multivariate Cox regression analyses of OS and RFS.

Please refer to the supplemented CD-ROM due to length of the table.

Table S5 RPPA data expression matrix with matched clinical data.

Please refer to the supplemented CD-ROM due to length of the table.

Table S6 Cl Score data matrix.

Please refer to the supplemented CD-ROM due to length of the table.

List of Abbreviations

ACC	Acetyl-CoA Carboxylase Alpha
AKT	Protein kinase B
ANOVA	Analysis of variance
ARG2	Arginase 2
ARNT	Aryl Hydrocarbon Receptor Nuclear Translocator
ASCT2	Solute Carrier Family 1 Member 5
ASL	Argininosuccinate Lyase
ASS1	Argininosuccinate Synthase 1
AT	Austria
ATCC	American Type Culture Collection
ATP	Adenosine triphosphate
BC	Breast cancer
BRAF	B-Raf Proto-Oncogene
CAD	Carbamoyl-Phosphate Synthetase 2
CH	Switzerland
CI	Confidence interval
Cl Score	Cell line Score
CPS1	Carbamoyl-Phosphate Synthase 1
DCA	Dichloroacetate
DE	Germany
DKFZ	Deutsches Krebsforschungszentrum
DNA	Deoxyribonucleic acid
ELISA	Enzyme-linked immunosorbent assay
EPO	Erythropoietin
ER	Estrogen receptor
FASN	Fatty Acid Synthase
FDG-PET	2-(18F)-fluoro-2-deoxyD-glucose positron emission tomography
FDR	False-discovery rate
FH	Fumarate Hydratase
G1	Gap 1
GAPDH	Glyceraldehyde-3-Phosphate Dehydrogenase
GBM	Glioblastoma multiforme

GLK	Glucokinase
GLS	Glutaminase
GLUD	Glutamate Dehydrogenase
GLUL	Glutamate-Ammonia Ligase
GLUT	Solute Carrier Family 2 Member
GOT1	Glutamic-Oxaloacetic Transaminase 1
GPT2	Alanine Aminotransferase 2
GSH	Glutathione
HER2	Human epidermal growth factor receptor 2
HIF	Hypoxia Inducible Factor
HR	Hazard ratio
HR	Hormone receptor
HRE	Hypoxia response element
IHC	Immunohistochemistry
IDH	Isocitrate Dehydrogenase
IgG	Immunoglobulin G
LAT1	Solute Carrier Family 7 Member 5
LDHA	Lactate Dehydrogenase A
LDHB	Lactate Dehydrogenase B
LRM	Linear regression model
MCT4	Monocarboxylate transporter 4
METABRIC	Molecular Taxonomy of Breast cancer International Consortium
MRM	Multiple reaction monitoring
mTORC1	Mammalian target of rapamycin complex 1
N	Node
Na	Sodium
NADH	Nicotinamide adenine dinucleotide
NAGS	N-Acetylglutamate Synthase
OAA	Oxaloacetic acid
ODC1	Ornithine Decarboxylase 1
OS	Overall survival
OXPHOS	Oxidative phosphorylation
p53	Tumor Protein P53
PAM	Prediction Analysis of Microarray
PCK	Phosphoenolpyruvate Carboxykinase

PD-1	Programmed cell death protein 1
PDH	Pyruvate Dehydrogenase
PDK	Pyruvate dehydrogenase kinase
pH	Potential of hydrogen
PHD	Prolyl hydroxylase
PHGDH	Phosphoglycerate Dehydrogenase
PI3K	Phosphatidylinositol-4,5-Bisphosphate 3-Kinase
PKM	Pyruvate Kinase, Muscle
pO_2	Partial pressure
PR	Progesterone receptor
PSAT1	Phosphoserine Aminotransferase 1
PSPH	Phosphoserine Phosphatase
PVDF	Polyvinylidene difluoride
RFS	Recurrence-free survival
RNA	Ribonucleic acid
ROS	Reactive oxygen species
RPPA	Reverse Phase Protein Array
RT	Room temperature
SD	Standard deviation
SDHA	Succinate Dehydrogenase Complex
SDS-PAGE	Sodium dodecyl sulfate polyacrylamide gel electrophoresis
SHMT2	Serine Hydroxymethyltransferase 2
SLC14A1	Urea Transporter 1
SMS	Spermine Synthase
SREBP1	Sterol Regulatory Element Binding Transcription Factor 1
SSR	Summed square of residuals
STARD10	StAR Related Lipid Transfer Domain Containing 10
STEEP	standardized definitions for efficacy end points
STRING	Search Tool for the Retrieval of Interacting Genes/Proteins
T	Tumor
TAC	Thesis advisory committee
TCA	Tricarboxylic acid cycle
TCGA	The Cancer Genome Atlas
TNBC	Triple negative
TNM	Tumor, Node, Metastasis

TW	Taiwan
UICC	International Union Against Cancer
UK	United Kingdom
US	United states of America
VEGFA	Vascular endothelial growth factor A
VHL	Von Hippel-Lindau